Dopaminergic Inputs in the Dentate Gyrus Direct the Choice of Memory Encoding

Huiyun Du^{a,1}, Wei Deng^{b,1}, James B. Aimone^{c,1}, Minyan Ge^a, Sarah Parylak^b, Keenan Walch^b, Jonathan Cook^b, Wei Zhang^d, Huina Song^a, Liping Wang^d, Fred H. Gage^{b,2}, and Yangling Mu^{a,e,2}

^aDepartment of Physiology, School of Basic Medicine, Huazhong University of Science and Technology, Wuhan 430030, China

^bSalk Institute for Biological Studies, Laboratory of Genetics, 10010 North Torrey Pines Road, La Jolla, California 92037, USA

^cSandia National Laboratories, Data-driven and Neural Computing Department, 1515 Eubank SE, Albuquerque, New Mexico 87185-1327, USA

^dShenzhen Key Lab of Neuropsychiatric Modulation, CAS Center for Excellence in Brain Science,
Shenzhen Institutes of Advanced Technology, Chinese Academy of Sciences, Shenzhen 518055, China
^eInstitute of Brain Research, Collaborative Innovation Center for Brain Science, Huazhong University of
Science and Technology, Wuhan 430030, China

¹H.D., W.D. and J.B.A. contributed equally to this work.

²To whom correspondence should be addressed. Email: ymu@hust.edu.cn (Y.M.), gage@salk.edu (F.H.G.)

Keywords: dopamine, channelrhodopsin-2, theta oscillation, temporal difference learning

Abstract

Rewarding experiences are often well remembered, which is known to be dependent on dopamine modulation of the neural substrates engaged in learning and memory; however, it is unknown how and where in the brain dopamine signals bias episodic memory toward preceding rather than subsequent events. Here we found that photostimulation of channelrhodopsin-2-expressing dopaminergic fibers in the dentate gyrus induced a long-term depression of cortical inputs, diminished theta oscillations and impaired subsequent contextual learning. Computational modeling based on this dopamine modulation indicated an asymmetric associations of events occurring before and after reward in memory tasks. In subsequent behavioral experiments, pre-exposure of a natural reward suppressed hippocampus-dependent memory formation, with an effective time window consistent with the duration of dopamine-induced changes of dentate activity. Overall, our results suggest a novel mechanism by which dopamine enables the hippocampus to encode memory with reduced interference from subsequent experience.

Significance Statement

Reward boosts forms of learning and memory through dopamine-mediated neuromodulation in the brain. However, the influence of dopamine has been an underappreciated component of episodic information in the hippocampus. Employing a cross-disciplinary approach, we demonstrate that dopaminergic input in the dentate gyrus, a hippocampal subregion critical for the formation of high-resolution memories, impairs subsequent learning by suppressing cortical inputs and ensemble neuronal activity in this area. This work reveals a novel mechanism by which dopamine signal biases memory storage of events leading to rather than subsequent to the reward.

Introduction

The brain structures crucial for memory formation are presumably under the control of the midbrain dopamine (DA) system, which selectively marks experiences that lead to reward (1, 2). In the striatum and the cortex, repetitive pairing of DA input after - but not before - sensorimotor stimulus within a narrow time window promotes structural and functional connectivity (3, 4), which may provide a cellular basis for reward to specifically reinforce an immediate past action. In the hippocampus, a structure that is instrumental in forming memories of contexts and objects making up the experiences (5, 6), DA must be present at the time of long-term potentiation (LTP) induction to increase the magnitude of early- and late-phase LTP (7-10). DA has also been found to enhance the reactivation of newly formed neural ensembles when released during learning (11). The requisite coincidence between the DA signal and the conditioning stimulation may serve to ensure that only inputs concurrent with or occurring shortly before reward are encoded in long-term memory. However, rewarding outcomes may often be delayed, and the involvement of the hippocampus is necessary when an event and its outcome are temporally discontinuous (12). This type of "memory" can be rapidly formed after even a single experience (5, 6), and behavioral studies demonstrate that application of DA agonists in the hippocampus hours after training promotes memory maintenance (13, 14), indicating that DA released from midbrain projections (Fig. S1) exerts distinct influences on the hippocampus to selectively reinforce memory of earlier events.

Here we surveyed the dentate gyrus (DG) of the hippocampus to explore the possible sites and actions of DA. As the first stage of the intrahippocampal trisynaptic loop, the DG receives multiple processed sensory inputs from the entorhinal cortex (EC) and uses conjunctive encoding to integrate them for a memory representation (15). This region, together with area CA3, has been shown to be active during new memory formation in humans (16-18). The DG is thought to transform noisy cortical

signals into sparse activation of distinct ensembles of granule cells (GCs) (19, 20), and this "pattern separation" function is indispensable for discrimination and storage of similar experiences (15, 21-23). The DG also displays numerous types of plastic processes that may underlie learning and memory in the hippocampus, including life-long generation of new neurons (24, 25). The DG thus possesses a special place in hippocampal anatomy and function. Because exogenously applied DA in slice preparations has been demonstrated to down-regulate GC excitation by cortical stimuli (26), we hypothesize that the DA system may impair post-reward learning, thereby allowing the preferential entry of information received before reward into the hippocampus.

Results

Electrophysiological and behavioral effects of optogenetic DA release in the DG

To investigate how DA release regulates DG activity *in vivo*, we adopted two strategies to produce animals with restricted expression of the light-gated ion channel channelrhodopsin-2 (ChR2) in dopaminergic neurons. First, we utilized offspring of tyrosine hydroxylase (TH)-Cre mice crossed with Ai27 mice bearing a Cre-dependent ChR2-tdTomato fusion gene. Their wild type (WT) littermates were used as control. Second, TH-Cre mice were transfected by injection of AAV-DIO-ChR2-mCherry or control AAV-DIO-mCherry viral vectors into the ventral tegmental area (VTA). The specificity and efficacy of Cre-dependent expression of ChR2 in TH-Cre;Ai27 and AAV-ChR2 mice were separately determined by co-localization of TH and tdTomato or mCherry (Fig. 1 A and B). Utilizing electrophysiological recordings from anesthetized animals, we confirmed that light stimulation delivered through an optic fiber in the VTA triggered a time-locked increase of phasic firing in most recorded

neurons expressing ChR2 (Fig. 1 C and D), although a small portion (8 of 51) displayed a decrease in spiking rate (data not shown). Since ChR2 was expressed not only in the soma but also in the axon (Fig. S2A), the optic fiber with electrodes affixed was moved to the DG to induce local DA release and to record GC activity (Fig. S2B). The electrophysiological readout revealed that field excitatory postsynaptic potentials (fEPSPs) evoked by electrical stimulation of the perforant path (PP) in TH-Cre;Ai27 mice were significantly decreased following 5-ms light exposure at 20 Hz for 5 minutes, with a kinetic profile similar to the long-term depression (LTD) caused by DA infusion into the DG of WT animals (Fig. 1 E and F). The same light stimulation induced an fEPSP reduction in the AAV-ChR2 group as well (Fig. 1G), but with a smaller amplitude and shorter duration as compared to the TH-Cre;Ai27 group (ANOVA: no significant group x time interaction, $F_{1,13} = 0.2815$, p = 0.9933; no significant time effect, $F_{13,111} = 0.429$, p = 0.9562; main group effect, $F_{1,111} = 11.65$, p = 0.0009), possibly due to differences in the number of ChR2-labeled dopaminergic cells and/or ChR2 expression levels.

The TH-Cre line has been reported to drive apparent non-dopaminergic expression patterns of Cre within VTA nuclei and a number of other brain structures, such as the locus coeruleus (LC) (27). It is thus possible that some ChR2-expressing fibers in the DG originated from noradrenergic nuclei in a TH-Cre;Ai27 mouse model. However, in line with most studies (28), norepinephrine (NE) potentiated GC responses elicited by PP stimulation, which was opposite to the effect of DA (Fig. S3A). We also quantified the colocalization between ChR2 and dopamine β-hydroxylase (DβH), a marker for noradrenergic neurons, and observed quite a low efficiency of Cre-dependent expression of ChR2 in the LC (Fig. S3 B and C). Taken together with similar LTD-like changes of fEPSPs following photostimulation in the TH-Cre;Ai27 and AAV-ChR2 groups (Fig. 1 E and G), these data suggested that activation of dopaminergic neurons in the VTA accounted for the synaptic change, although the

involvement of NE could not be completely excluded. To further validate the role of DA, we preinfused antagonists specifically targeting DA receptors, a mixture of D1-like receptor blocker SCH
23390 and D2-like receptor blocker sulpiride, into the DG of TH-Cre; Ai27 mice and found that lightinduced LTD of fEPSPs was fully abolished (Fig. 1H). This piece of evidence rules out the possible
action of GABA, if there was DA and GABA co-release from dopaminergic neurons as previously
documented (29, 30), and confirms that the effect of optogenetic manipulation was mediated by DA. It
is also noted that administration of DA antagonists itself elicited a small and steady increase in the
fEPSP amplitude (although not statistically significant, ANOVA: p = 0.1), indicating a possible impact
of tonic DA release on basal synaptic transmission in the DG.

Next, we performed bilateral DG photostimulation with unilateral DG recording in freely moving animals (Fig. S4). When the mice were allowed to freely behave in the home cage environment, theta frequency (4–12 Hz) oscillation of local field potentials (LFPs) could be frequently observed. Control WT littermates and AAV-mCherry mice did not show any significant light-induced LFP alterations at DG sites throughout the course of the experiment (Fig. 2 A and B). In contrast, LFP oscillatory powers in TH-Cre;Ai27 and AAV-ChR2 mice appeared to be reduced at most frequencies following the light stimulation epoch (Fig. 2 C and D). Spectral analysis of the last 10-min recording period (~20–30 minutes after delivery of light pulses) relative to the 10-min control period before stimulation showed that, in comparison to the controls, the LFP power change in the theta frequency range was significant in AAV-ChR2 mice. Similarly, a trend in LFP power reduction was observed in the TH-cre;Ai27 group, despite lack of statistical significance (Fig. 2E). Theta power and frequency may vary with the locomotion speed. To corroborate that the observed decrease in theta power was a result of optical stimulation rather than behavioral variability, we analyzed the data set of anesthetized animals included in Fig. 1. As shown in Fig. S5, light exposure resulted in a significant drop of theta

power in AAV-ChR2 mice in comparison to AAV-mCherry controls. TH-Cre; Ai27 mice also showed a trend towards theta power decrease as compared to their WT littermates, and this reduction of theta power could be fully prevented by DA receptor blockers. Thus, optical stimulation appeared to have similar effects on theta oscillations in anesthetized and freely behaving animals.

To evaluate whether the impact of DA was behaviorally relevant, we examined the performance of mice subject to optogenetic activation in a contextual fear conditioning paradigm that combined context pre-exposure with an immediate foot shock (31). Taking the DG's role in behavioral pattern separation into account, we not only measured the freezing behavior in the conditioned context (context A), but also assessed context discrimination by examining post-conditioning fear behaviors of mice in another context (context B) that was similar but not identical to context A (32). The TH-Cre; Ai27 mice that received photostimulation ~0.5 hr before context pre-exposure exhibited a tendency to freeze less in context A as compared to WT animals, whereas AAV-ChR2 mice subjected to optical stimulation appeared to show a slight but not statistically significant increase in the fear to context B than AAVmCherry mice (Fig. 2F). Despite this difference, both TH-Cre;Ai27 and AAV-ChR2 mice failed to distinguish context A from B, in contrast to the controls that underwent the same treatment paradigms and froze significantly more in context A than in context B (Fig. 2F). To quantify the difference between fear responses to the two environments, we computed a discrimination index, defined as freezing in context A minus freezing in context B. As shown in Fig. 2G, the discrimination index in the TH-Cre; Ai27 group was significantly lower than that in the WT group, and AAV-ChR2 mice had a lower discrimination index than AAV-mCherry controls. Since photostimulation did not alter exploratory behavior during context pre-exposure (Fig. S6), the pre-learning DA signal appeared to impair new memory formation, which was most obviously reflected by the compromised context discrimination ability.

To directly test the modulatory effect of DA, we infused DA into the DG prior to contextual preexposure. Consistent with the results of the optogenetic experiment, the DA-infused animals froze
considerably less in context A in comparison to the saline-infused controls. Furthermore, unlike the
control mice that could discriminate context A from context B, DA-infused mice did not display
significantly more freezing in context A than in context B, with a dramatically lower discrimination
index (Fig. 3A). However, their motility or explorative drive during context pre-exposure was not
altered (Fig. 3B). Thus, hippocampal DA infusion and optical stimulation of ChR2-expressing
dopaminergic axons in the DG exerted similar effects on contextual learning, demonstrating that the
memory of events occurring subsequent to the dopamine signal was stored less efficiently.

DA can impact temporal associations on dentate function

While the observation that optogentically-induced DA release induces a strong LTD effect is intriguing, it is unclear what the functional impact of this depression would be in natural behaviors since the role of DA in DG function has not been well explored. It is well accepted that the impact of DA in other regions can be thought of as temporal in nature, providing capabilities in reinforcement learning and consolidation. Likewise, we have previously hypothesized that the DG's population activity would exhibit strong temporal structure due to its mixed population of young and old GCs (33, 34), a prediction that has been observed in a series of behavioral and physiology studies (35, 36). We accordingly predicted that the suppression of DG activity after DA may interact non-trivially with these temporal associations produced by the DG.

To explore whether DA-LTD could impact temporal coding in the DG after a reward, we implemented DA modulation in a computational model consisting of a highly abstracted, two-layer feed forward network where the output layer gradually added neurons (Fig. 4A). At a set time, DA was

modeled by reducing the synaptic strengths of excitatory inputs as demonstrated in Fig. 1. Not surprisingly, DA-LTD sharply suppressed the activity of the outputs (Fig. 4 B and C), and this suppression had a marked effect on the correlations between the model's outputs. Without DA, events close to one another in presentation time had increased correlations, an effect we described previously as "pattern integration" (34). These associations were typically symmetrical in time; a given event was equally likely to be associated with a preceding event as with a following event (Fig. 4D). However, the presence of DA disrupted this symmetry; if DA was released after an event, its associations were biased towards those other events that preceded it (Fig. 4 E and F). Similarly, events that occurred after DA release were associated preferentially with other post-reward events (Fig. 4G). The results from this simulation thus propose a role for DA in the DG similar to temporal difference learning (TDL) at the long time scales relevant for declarative memory encoding, and suggest that experience-dependent DA release could significantly impact hippocampal-dependent learning in a temporally asymmetric manner.

We then examined whether a positive deflection of PP strength, which is a potential impact of NE signaling (Fig. S3), would produce a similar asymmetry in this simple model (Fig. S7 A-D). Because our model was highly abstract, and thus lacks known hilar inhibitory feedback that is known to normalize substantial positive deflections of DG activity, we considered only moderate increases in PP strength as a model of NE. While an increase of PP strength indeed impacted the associations in our modeled DG, the effect was predominately isolated to the temporal window of NE potentiation, with minimal impact on associations between pre- and post-perturbed activity (Fig. S7 E-F).

Impairment of spatial memory by pre-learning reward

To investigate if optogenetic control mimicked the presence of a natural reward, we gave WT mice sweetened condensed milk as reward instead of light pulses before context pre-exposure during the

fear conditioning procedure. In contrast to the controls that were given water, the mice that received the milk reward ~1 hr before pre-exposure to the conditioning context showed remarkably less fear response in context A and were compromised in the discrimination of context A from context B, as indicated by a significant drop in the discrimination index (Fig. 5A). This finding is consistent with the result of the photostimulation experiment that indicated a DA-induced decrement in learning (Fig. 2) and the observation of impaired correlations in the computational model (Fig. 4). However, a milk reward provided to a new cohort of mice 6 hr before the contextual pre-exposure had no effect on contextual memory (Fig. 5B), suggesting that the behavioral effect of the reward was transient. Moreover, the impaired memory formation was not detected in mice given the reward at other time points during the behavioral procedure, including immediately after context pre-exposure, before immediate shock and before memory test (Fig. S8), suggesting that the reward signal influenced the information acquisition during pre-exposure rather than altering shock perception or the later association of context information with shock. Importantly, this experiment also ruled out the possibility that the reward led to a positive association with context A on the day of pre-exposure and thus to less freezing behavior when a shock was presented in the same environment the next day. Finally, we did not detect any significant effect of milk reward on the motility and exploration of mice in either the open field test or contextual preexposure (Figs. S9 and S10), indicating that the behavioral phenotype was not caused by an indirect effect of reward on motor activity and/or explorative drive. Hence, the pre-learning DA increase resulted in a transient deficit in memory formation.

We next examined how a reward received shortly before training would affect learning a new spatial location in a Barnes maze. We first trained mice for one target location in the maze and then divided the animals into two groups, with one group receiving a sweetened milk reward and the other group getting water as control. About 0.5–1 hr after the reward, both groups were trained to learn a new

target position that was located 90 degrees from the original position (Fig. 5C). Compared to the control group, mice in the reward group made significantly more errors, took significantly more time, and traveled significantly longer to find the new target location (Fig. 5D). In contrast, no significant difference was detected in the navigational speed between the reward and control groups (Fig. 5E), suggesting that the reward had no effect on the general motility of the animals. These data corroborated the finding that a reward received shortly before learning had a detrimental effect on memory.

Natural reward occludes the in vitro effect of DA

To verify the correlation between a pre-learning reward-induced impairment in memory tasks and the electrophysiological effect of DA on the DG, we examined the action of DA perfusion in brain slices prepared from mice that were fed sweetened condensed milk immediately before sacrifice (Fig. 6A), based on the observation that DA-induced LTD at PP-GC synapses was saturated by a single episode of drug administration (Fig. 6B). In slices obtained from milk-treated animals when the recordings were made 2-4 hr but not over 4 hr after milk delivery, an ensuing DA perfusion failed to generate any further depression in GCs, including in those born during adulthood (Fig. 6C-F). Consistent with our prior finding that activation of D2- but not D1-like receptors mediated DA-LTD upon neuronal maturation (26), pre-injection of sulpiride completely overcame the occlusion effect of reward on mature GCs, whereas milk reward preceded by injection of SCH 23390 still significantly diminished subsequent LTD triggered by exogenous DA (Fig. 6G). Therefore, natural DA system activation triggered PP-GC synaptic changes that closely resembled LTD induced by in vitro DA application, with a duration largely fitting with behavioral assessments. It is very likely that DAinduced LTD in new and old neurons was dependent on D1- and D2-like receptor-mediated signaling, respectively (26).

DA regulation in distinct hippocampal subfields

To further confirm the involvement of DG in the pre-reward-induced learning deficit, we analyzed DA regulation in the other hippocampal subareas. We first made extracellular field recordings from Schaffer collaterals (SC) and temporoammonic (TA) pathways to field CA1 (Fig. 7A). Consistent with previous reports (37, 38), DA suppressed fEPSPs evoked by TA stimulation for a short period but did not significantly alter the transmission at SC-CA1 synapses (Fig. 7B). Similarly, in the CA3 region, DA administration led to a transient reduction in fEPSPs evoked by PP projections, whereas no significant changes were detected in recurrent excitation via the extensive network of associational/commissural (A/C) connections among CA3 pyramidal cells (Fig. 7C). In contrast, field responses at PP-DG synapses were decreased to a level similar to what has been demonstrated in individual GCs by whole-cell patch-clamp recordings (Fig. 7D). As summarized in Fig. 7E, only the inhibition occurring in the DG was long-lasting, although the levels of depression in distinct hippocampal subregions were not significantly different. To determine whether in vivo DA release produced a short-term depression (STD) in CA1 as in vitro, we recorded TA-evoked fEPSPs from brain slices of mice pre-rewarded with milk as in Fig. 6A. As predicted, DA applied to the bathing solution 2–4 hr after milk treatment resulted in an STD almost identical to that in slices from control animals (Fig. 7F), indicating that food reward did not occlude ex vivo LTD in CA1 as in the DG. Taken together, our data indicate that the long duration of the DA effect appeared to be a unique feature of the DG and, in this regard, DA modulation of DG activity was more likely to underlie the behavioral changes shown in Figs. 3 and 5. Since DA receptors show a higher abundance and diversity in the DG than in the other hippocampal subareas (26), we speculate that the observed differential effects of DA in distinct hippocampal subfields may be caused by different levels and/or combinations of DA receptors.

Discussion

To date, most studies characterizing the role of DA in hippocampal learning have focused on the CA1 region. For instance, DA has been demonstrated to enhance LTP, especially late LTP at SC-CA1 synapses when present at the time of induction (10), indicating a mechanism by which information arriving coincident with or right before reward could be recorded into persistent memory by the hippocampus. But several important issues remain unknown: first, how can reward facilitate memory of events occurring hours beforehand? Second, are memories more readily formed or simply prolonged in the presence of reward? Third, are memories influenced by DA's actions on hippocampal subregions other than CA1? In this study, we reveal an effect of DA on DG activity within a long time window after reward. By globally reducing excitation of GCs (Fig. 1), DA may drive the DG to filter out weak stimuli and to incorporate fewer inputs during "conjunctive encoding" (15), which probably leads to memory containing less information or possessing low "resolution" (33). Furthermore, we found that the pre-stimulus theta rhythm was weakened after DA release (Figs. 2 and S5). Although the function of theta oscillation is not clearly understood yet, prior studies have suggested its importance in mnemonic information encoding, as it reflects the "on-line" state or a state of readiness to process incoming signals in the hippocampus (39). It has been demonstrated that the amplitude of hippocampal oscillations before stimulus onset, especially in the theta range, is positively correlated with later episodic memory formation (40, 41). Here we suggest that the reduction of theta power may reflect disruption of hippocampal ensemble activity and therefore altered neuronal encoding. Indeed, our behavioral tests demonstrate that pre-learning optical activation of VTA impairs memory of a specific context in which

animals receive one-trial contextual fear conditioning (Fig. 2). We noted that TH-Cre; Ai27 mice exhibit a tendency to freeze less in context A, whereas AAV-ChR2 mice display a tendency to freeze more in context B (Fig. 2F). A possible explanation for the difference between these two groups is that photostimulation seems to generate a weaker impact on both fEPSP and theta oscillation in AAV-ChR2 mice than in TH-Cre; Ai27 mice (Figs. 1, 2 and S5). As a consequence, AAV-ChR2 mice can form the memory of context A but with some details missing, thereby failing to differentiate context B from A. In contrast, TH-Cre; Ai27 mice tend to ignore more information and therefore fail to remember context A at all. These results suggest that pre-learning DA signal primarily impairs the ability to discriminate the training context and a similar environment. We further reveal an effect of natural reward similar to that of optogenetic manipulation (Fig. 5), and the reward can affect animal behavior within a long time window, which is in accordance with the key feature of long-lasting variation of neural activity associated with DA modulation in the DG (Figs. 6 and 7). Thus, our findings indicate an important role for the DG in the mediation of brain responsiveness to rewarding stimuli. It is possible that incoming information can be retained by default, unless prevented by a preceding DA signal. In this way, DA reduces interference from inputs arriving after a reward and increases the contrast between events taking place before and after reward; thereby virtually favoring the entrance of information temporally prior to reward into the hippocampus, be it a long time or shortly before reward. Complementing previous studies revealing that the midbrain DA system serves to stabilize memory of events coincident with reward by promoting CA1 late LTP and network dynamics (10, 11), the present study provides a mechanism by which information acquired before reward is more readily encoded into memory as compared to that acquired after reward, particularly when the input and DA signal are temporally discontinuous.

The DG has been identified as a major neurogenic region in the adult brain, and increasing evidence suggests that newborn neurons contribute to hippocampus-related learning and memory (33). Although the specific function of newly generated GCs in these processes remains elusive, they might work through two mechanisms that are not mutually exclusive. First, the plastic properties of immature GCs could allow them to participate in information storage per se, given prior findings that adultgenerated GCs form a critical and enduring component of hippocampal memory traces (42, 43). Second, newborn GCs could introduce a degree of similarity to memories learned at the same time, a process referred to as "pattern integration" (34). They could be particularly important in combining inputs from various sources to form a complete representation of a context or an event. Thus, DA-induced suppression of neural transmission to these neurons could hinder the "conjunctive encoding" of the context, resulting in contextual discrimination deficits. Although further study is required to address whether young GCs play an identical or different role as their older counterparts, our results provide in *vivo* evidence that adult-generated neurons are indeed integrated into the broad hippocampal circuitry composed of subcortical modulatory systems (Fig. 6 E and F). The computational modeling of the DG network with continuous addition of new neurons suggests that events occurring prior to DA release show stronger correlations with temporally proximal events without DA (Fig. 4), causing a retroactive bias in the temporal relationships if there is more DA for later events compared to earlier ones. Such a function for DA has been suggested in a number of other regions for more immediate reward-based learning (44). At neurogenesis time scales, one perspective of this TDL function would be that, for very large rewards, DA in the DG could serve to separate episodic parts of memory into predictive components (Fig. 4E). Events in life would, in a sense, be binned together to represent episodes that lead to significant rewards; what happens post-reward is only important with regard to the next rewarding event. Even smaller rewards, with smaller relative effects of DA, would be valuable in

encoding causation into memory associations. One of the observations from our computational model is that DA in the DG interacts with the unique memory functions of adult-born neurons, a result consistent with their differential expression of DA receptors (26). As techniques for targeting specific ages of young neurons are further developed, it will be interesting to dissociate their contribution to our observed behavioral results.

Materials and Methods

Detailed methods are provided in *Supporting Information*. Briefly, TH-Cre transgenic mice were crossed with Ai27 mice or injected with AAV to express ChR2 in their dopaminergic neurons.

Photostimulation (5-ms pulses at 20/50 Hz) was applied through the optical fiber connected to a blue laser (λ = 473 nm). The laser power intensity was kept constant at ~13 mW for reliable activation of ChR2 in DA neurons. A bundle of four or eight tetrodes were used for recording LFPs in the DG. Time-frequency decomposition was performed for LFP signals obtained before and after optical stimulation from both freely moving and anesthetized animals. Mice subjected to photostimulation were used for fear conditioning tests. C57BL/6 mice pre-treated with milk were used for fear conditioning or Barnes maze tests. Replication-incompetent retroviruses expressing GFP were prepared and injected into the DG of 6- to 7-week-old female C57BL/6 mice. At 4–6 weeks post infection (wpi), acute brain slices were obtained from animals pre-treated with water or milk, and whole-cell patch-clamp recordings were made from GFP-expressing GCs and their non-labeled neighbors. Age-matched animals without virus injection were used for extracellular field recordings. Computational simulations were performed on an abstract two-layer neural network model, in which DA modulation was simulated by decreasing activity

of EC inputs by a variable fraction. All values are reported as mean \pm SEM, unless indicated otherwise. Statistical significance was determined by Student's t-test and two-way repeated-measures ANOVA for electrophysiology and behavioral data, respectively.

Author Contributions

Y.M., W.D., J.B.A. and F.H.G. contributed to the study design and the manuscript writing. H.D., with help from Y.M., performed all *in vivo* recordings and the behavior test with optogenetic manipulation and analyzed the data. W.D. conducted all other behavioral studies. Y.M. and M.G. conducted all *in vitro* electrophysiology studies. J.B.A. conducted the computational modeling experiment. S.P. and K.W. contributed to the Barnes maze test. J.C. assisted in behavioral assays. W.Z. and H.S. performed the immunostaining experiments. L.W. provided technical support for the optogenetic studies.

Acknowledgments

We thank C. Burger for technical assistance, X. Jin and S. Small for comments on this manuscript, M.L. Gage for editorial comments, and J. Simon for help with illustrations. This work was supported by National 1000-Young-Talent Program of China, the Fundamental Research Funds for the Central Universities, HUST: 2014TS059 and the National Natural Science Foundation of China 91332106 to Y. Mu, the James S McDonnell Foundation, Mather's Foundation, NIMH, Ellison Foundation, and JPB Foundation to F. H. Gage, and LDRD program support from Sandia National Laboratories to J. B.

Aimone. Sandia National Laboratories is a multi-program laboratory managed and operated by Sandia Corporation, a wholly owned subsidiary of Lockheed Martin Corporation, for the U.S. Department of Energy's National Nuclear Security Administration under contract DE-AC04-94AL85000.

References

- 1. Shohamy D & Adcock RA (2010) Dopamine and adaptive memory. *Trends in cognitive sciences* 14(10):464-472.
- 2. Wise RA (2004) Dopamine, learning and motivation. *Nature reviews. Neuroscience* 5(6):483-494.
- 3. Bao S, Chan VT, & Merzenich MM (2001) Cortical remodelling induced by activity of ventral tegmental dopamine neurons. *Nature* 412(6842):79-83.
- 4. Yagishita S, *et al.* (2014) A critical time window for dopamine actions on the structural plasticity of dendritic spines. *Science* 345(6204):1616-1620.
- 5. Burgess N, Maguire EA, & O'Keefe J (2002) The human hippocampus and spatial and episodic memory. *Neuron* 35(4):625-641.
- 6. Squire LR, Stark CE, & Clark RE (2004) The medial temporal lobe. *Annual review of neuroscience* 27:279-306.
- 7. Frey U, Huang YY, & Kandel ER (1993) Effects of cAMP simulate a late stage of LTP in hippocampal CA1 neurons. *Science* 260(5114):1661-1664.
- 8. Hamilton TJ, et al. (2010) Dopamine modulates synaptic plasticity in dendrites of rat and human dentate granule cells. Proceedings of the National Academy of Sciences of the United States of America 107(42):18185-18190.
- 9. Lemon N & Manahan-Vaughan D (2006) Dopamine D1/D5 receptors gate the acquisition of novel information through hippocampal long-term potentiation and long-term depression. *The Journal of neuroscience : the official journal of the Society for Neuroscience* 26(29):7723-7729.
- 10. Lisman J, Grace AA, & Duzel E (2011) A neoHebbian framework for episodic memory; role of dopamine-dependent late LTP. *Trends in neurosciences* 34(10):536-547.
- 11. McNamara CG, Tejero-Cantero A, Trouche S, Campo-Urriza N, & Dupret D (2014) Dopaminergic neurons promote hippocampal reactivation and spatial memory persistence. *Nature neuroscience*.
- 12. Foerde K & Shohamy D (2011) Feedback timing modulates brain systems for learning in humans. *The Journal of neuroscience : the official journal of the Society for Neuroscience* 31(37):13157-13167.
- 13. Bernabeu R, *et al.* (1997) Involvement of hippocampal cAMP/cAMP-dependent protein kinase signaling pathways in a late memory consolidation phase of aversively motivated learning in rats. *Proceedings of the National Academy of Sciences of the United States of America* 94(13):7041-7046.

- 14. Rossato JI, Bevilaqua LR, Izquierdo I, Medina JH, & Cammarota M (2009) Dopamine controls persistence of long-term memory storage. *Science* 325(5943):1017-1020.
- 15. Kesner RP (2007) A behavioral analysis of dentate gyrus function. *Progress in brain research* 163:567-576.
- 16. Eldridge LL, Engel SA, Zeineh MM, Bookheimer SY, & Knowlton BJ (2005) A dissociation of encoding and retrieval processes in the human hippocampus. *J Neurosci* 25(13):3280-3286.
- 17. Suthana N, Ekstrom A, Moshirvaziri S, Knowlton B, & Bookheimer S (2011) Dissociations within human hippocampal subregions during encoding and retrieval of spatial information. *Hippocampus* 21(7):694-701.
- 18. Zeineh MM, Engel SA, Thompson PM, & Bookheimer SY (2003) Dynamics of the hippocampus during encoding and retrieval of face-name pairs. *Science* 299(5606):577-580.
- 19. Chawla MK, *et al.* (2005) Sparse, environmentally selective expression of Arc RNA in the upper blade of the rodent fascia dentata by brief spatial experience. *Hippocampus* 15(5):579-586.
- 20. Jung MW & McNaughton BL (1993) Spatial selectivity of unit activity in the hippocampal granular layer. *Hippocampus* 3(2):165-182.
- 21. Bakker A, Kirwan CB, Miller M, & Stark CE (2008) Pattern separation in the human hippocampal CA3 and dentate gyrus. *Science* 319(5870):1640-1642.
- 22. Leutgeb JK, Leutgeb S, Moser MB, & Moser EI (2007) Pattern separation in the dentate gyrus and CA3 of the hippocampus. *Science* 315(5814):961-966.
- 23. McHugh TJ, *et al.* (2007) Dentate gyrus NMDA receptors mediate rapid pattern separation in the hippocampal network. *Science* 317(5834):94-99.
- 24. Derrick BE (2007) Plastic processes in the dentate gyrus: a computational perspective. *Prog Brain Res* 163:417-451.
- 25. Lledo PM, Alonso M, & Grubb MS (2006) Adult neurogenesis and functional plasticity in neuronal circuits. *Nat Rev Neurosci* 7(3):179-193.
- 26. Mu Y, Zhao C, & Gage FH (2011) Dopaminergic modulation of cortical inputs during maturation of adult-born dentate granule cells. *The Journal of neuroscience : the official journal of the Society for Neuroscience* 31(11):4113-4123.
- 27. Lammel S, *et al.* (2015) Diversity of transgenic mouse models for selective targeting of midbrain dopamine neurons. *Neuron* 85(2):429-438.
- 28. Harley CW (2007) Norepinephrine and the dentate gyrus. *Progress in brain research* 163:299-318.
- 29. Maher BJ & Westbrook GL (2008) Co-transmission of dopamine and GABA in periglomerular cells. *Journal of neurophysiology* 99(3):1559-1564.
- 30. Tritsch NX, Ding JB, & Sabatini BL (2012) Dopaminergic neurons inhibit striatal output through non-canonical release of GABA. *Nature* 490(7419):262-266.
- 31. Fanselow MS (2000) Contextual fear, gestalt memories, and the hippocampus. *Behavioural brain research* 110(1-2):73-81.
- 32. Deng W, Mayford M, & Gage FH (2013) Selection of distinct populations of dentate granule cells in response to inputs as a mechanism for pattern separation in mice. *eLife* 2:e00312.
- 33. Aimone JB, Deng W, & Gage FH (2011) Resolving new memories: a critical look at the dentate gyrus, adult neurogenesis, and pattern separation. *Neuron* 70(4):589-596.
- 34. Aimone JB, Wiles J, & Gage FH (2009) Computational influence of adult neurogenesis on memory encoding. *Neuron* 61(2):187-202.
- 35. Kesner RP, *et al.* (2014) The role of postnatal neurogenesis in supporting remote memory and spatial metric processing. *Hippocampus* 24(12):1663-1671.

- 36. Rangel LM, *et al.* (2014) Temporally selective contextual encoding in the dentate gyrus of the hippocampus. *Nature communications* 5:3181.
- 37. Ito HT & Schuman EM (2007) Frequency-dependent gating of synaptic transmission and plasticity by dopamine. *Frontiers in neural circuits* 1:1.
- 38. Otmakhova NA & Lisman JE (1999) Dopamine selectively inhibits the direct cortical pathway to the CA1 hippocampal region. *The Journal of neuroscience : the official journal of the Society for Neuroscience* 19(4):1437-1445.
- 39. Buzsaki G (2002) Theta oscillations in the hippocampus. *Neuron* 33(3):325-340.
- 40. Berry SD & Thompson RF (1978) Prediction of learning rate from the hippocampal electroencephalogram. *Science* 200(4347):1298-1300.
- 41. Guderian S, Schott BH, Richardson-Klavehn A, & Duzel E (2009) Medial temporal theta state before an event predicts episodic encoding success in humans. *Proceedings of the National Academy of Sciences of the United States of America* 106(13):5365-5370.
- 42. Arruda-Carvalho M, Sakaguchi M, Akers KG, Josselyn SA, & Frankland PW (2011) Posttraining ablation of adult-generated neurons degrades previously acquired memories. *The Journal of neuroscience : the official journal of the Society for Neuroscience* 31(42):15113-15127.
- 43. Deng W, Saxe MD, Gallina IS, & Gage FH (2009) Adult-born hippocampal dentate granule cells undergoing maturation modulate learning and memory in the brain. *The Journal of neuroscience : the official journal of the Society for Neuroscience* 29(43):13532-13542.
- 44. Schultz W, Dayan P, & Montague PR (1997) A neural substrate of prediction and reward. *Science* 275(5306):1593-1599.

Figure Legends

- **Fig. 1.** Optical stimulation of dopaminergic terminals in the DG induces LTD-like changes at PP-DG synapses
- (A) Representative images showing co-expression of ChR2-mCherry and TH in the VTA of TH-Cre mice infected with AAV-DIO-ChR2-mCherry.
- (B) Quantification showing the overlap of ChR2+TH+ cells with TH+ or ChR2+ cells in the VTA (from seven TH-cre; Ai27 mice and seven AAV-ChR2 mice). Error bars, SEM.
- (C) Typical superimposed spike waveforms of one ChR2-expressing neuron in the VTA activated by blue light. Scales: $20~\mu V$ and $200~\mu S$.
- (D) Single-unit recordings in the VTA. The raster plot (top) shows the spike times for 5 optical stimulation trials (473 nm, 5 ms, 20 Hz). The peristimulus time histogram (bottom) shows the averaged response across all repetitions (50 ms bins).
- (E) Summary data of the effects of light stimulation (5-ms pulses at 20Hz for 5 minutes; black bar) in the DG of TH-cre; Ai27 mice and their control littermates (ANOVA: p < 0.0001; TH-cre; Ai27: n = 7, WT: n = 4). Data represent the fEPSP amplitudes normalized by the mean values before optical stimulation and averaged over 2-min bins for each experiment. Error bars, SEM.
- (F) Summary plot of changes in fEPSPs evoked by PP stimulation after DA or vehicle (Veh) infusion (black bar) into the DG of WT animals (ANOVA: p < 0.0001; DA: n = 11, Veh: n = 8). Data represent the fEPSP amplitudes normalized by the mean values before DA or Veh infusion and averaged over 2-min bins for each experiment. Error bars, SEM.
- (G) Summary data of the effects of light stimulation (5-ms pulses at 20Hz for 5 minutes; black bar) in the DG of TH-cre mice infused with AAV-ChR2 or control viral vectors (ANOVA: p < 0.0001; AAV-ChR2: n = 5, AAV-mCherry: n = 6). Data are presented in the same manner as in (E).

- (H) Photostimulation (black bar) following infusion of DA receptor antagonists (red bar) into the DG does not induce significant changes in the fEPSP amplitude (n = 7). Data presented as in (E).
- **Fig. 2.** Pre-learning optical stimulation causes changes in DG network oscillations and impairs memory formation
- (A) Averaged power spectrogram of LFPs in WT littermates exposed to light stimulation (n = 9). White curve indicates the total power of the theta band LFP signal (4–12 Hz). Dashed lines mark the time of blue light delivery (5-ms pulses at 20 Hz for 5 minutes). Horizontal white bars mark the time periods used for quantitative comparison of LFP powers between 4 and 12 Hz.
- (B) Averaged power spectrogram of LFPs in TH-Cre mice transduced with AAV-DIO-mCherry exposed to light stimulation (n = 11). Data presented as in (A).
- (C) Averaged power spectrogram of LFPs in TH-cre; Ai27 mice exposed to light stimulation (n = 8). Data presented as in (A).
- (D) Averaged power spectrogram of LFPs in TH-Cre mice transduced with AAV-DIO-ChR2-mCherry exposed to light stimulation (n = 11). Data presented as in (A).
- (E) Histogram showing LFP power (4–12 Hz) change measured during interval indicated in (A) relative to 10-min baseline segment before stimulation (t-test: TH-cre;Ai27 vs. WT, p = 0.12; AAV-ChR2 vs. AAV-mCherry, p = 0.02). *p < 0.05.
- (F) Control but not TH-cre; Ai27 mice undergoing photostimulation before context pre-exposure freeze significantly longer in context A than in context B (ANOVA: group x context interaction, $F_{1,17} = 7.069$, p = 0.0165; post hoc for WT vs. TH-cre; Ai27, context A, p > 0.05; context B, p > 0.05; post hoc for context A vs. context B: WT, p < 0.001, n = 10; TH-cre; Ai27, p > 0.05, n = 9). In comparison to the AAV-mCherry group, AAV-ChR2 mice freeze similarly in context A and B (ANOVA: group x context interaction, $F_{1,21} = 6.160$, p = 0.0216; post hoc for AAV-mCherry vs. AAV-ChR2, context A, p > 0.05;

context B, p > 0.05; post hoc for context A vs. context B: AAV-mCherry, p < 0.001, n = 12; AAV-ChR2, p > 0.05, n = 11). ***p < 0.001.

- (G) The discrimination index is significantly lower in the TH-cre; Ai27 and AAV-ChR2 groups than in their respective control group (t-test: WT vs. TH-cre; Ai27, $t_{17} = 2.609$, p = 0.018; AAV-mCherry vs. AAV-ChR2, $t_{21} = 2.482$, p = 0.022). *p < 0.05.
- Fig. 3. Pre-training elevation of the hippocampal DA level is sufficient to cause a learning deficit (A) Top, experimental scheme. On the first day, mice were infused with DA and allowed to explore context A ~1 hr later. The next day, mice received an immediate foot shock in context A'. The fear behavior of mice was then tested in context A and B in a counter-balanced order. Bottom, infusion of DA into the hippocampus before training causes a deficit in learning. The mice infused with control solution but not with DA freeze more in context A than in context B (ANOVA: group x context interaction, $F_{1,21} = 5.134$, p = 0.035; post hoc for control vs. DA, context A, p < 0.05; context B, p > 0.05; post hoc for context A vs. context B: control group, p < 0.001, p = 12; DA group, p > 0.05, p = 11. The discrimination index is significantly lower in the DA group compared to the control group (t-test, p = 0.035). Data are presented as mean p = 0.035. Data are presented as mean p = 0.035. Bata are presented as mean p = 0.035. The average motion of the mice that were infused with DA 1 hr before pre-exposure is not significantly different
- motion of the mice that were infused with DA 1 hr before pre-exposure is not significantly different from that of the control mice (ANOVA: no significant DA x time interaction, $F_{1,9} = 0.5464$, p = 0.83; no significant DA effect, $F_{1,189} = 1.390$, p = 0.25; main time effect, $F_{9,189} = 4.461$, p < 0.0001; DA group, p = 11; Veh group, p = 12.
- Fig. 4. Implementation of DA in a simple neurogenic two-layer neural network
- (A) Schematic of model. The neural network consists of an input layer of excitatory and inhibitory neurons and a neurogenic second layer that is initialized with no neurons. At each time step, the network

is trained with a new event and two immature neurons are added to the network. At time steps 65 through 70 (shaded green), DA is added to the network. Each plot below represents an average of 5,000 model runs.

- (B) DA (presented during shaded events) suppresses model output considerably. Even a relatively weak effect on excitatory synapses can greatly suppress network activity.
- (C) Strong DA suppression limits the population of responding neurons to only a subset of the youngest neurons in the network. Inactivity above diagonal is indicative of neurons not being born yet.
- (D) Cross-similarity plot of network encoding of events without DA; events are associated symmetrically in time due to neurogenesis.
- (E) Cross-similarity plot of network encoding of events with strong DA during events 65–70. Pre-DA and post-DA events are encoded using essentially distinct populations of neurons.
- (F) Events preceding DA are temporally associated with one another but show greatly reduced associations with events during (shaded area) and after DA.
- (G) Events following DA (shaded area) are temporally associated with other post-DA events. In (F) and (G), note the symmetry of associations in the non-DA condition (blue).

Fig. 5. Natural reward transiently impairs spatial memory formation

- (A) Appetitive reward treatment 1 hr before training causes compromised learning. Control mice display significantly more freezing behavior in context A than the milk-treated mice (ANOVA: group x context interaction, $F_{1,39} = 6.966$, p = 0.012; post hoc: context A, p < 0.05, context B, p > 0.05; water group, n = 20; milk group, n = 21). Milk-treated mice have a significant lower discrimination index compared to the control mice (t-test, $t_{39} = 2.069$, p = 0.045). * indicates statistically significant.
- (B) Reward treatment 6 hr before training has no effect on learning. Both groups of mice show significantly more freezing behavior in context A than in context B (ANOVA: group x context

interaction, $F_{1,40} = 2.641$, p = 0.11; n = 21 in each group). There is no significant difference in the discrimination index between milk-treated mice and the control mice (t-test, $t_{40} = 1.625$, p = 0.11). * indicates statistically significant.

- (C) Experimental scheme of Barnes maze experiment.
- (D) Milk-treated mice are impaired in reversal learning compared to control mice. Left top, errors made before reaching the target location (two-way ANOVA: group effect, $F_{1,45} = 6.077$, p = 0.0176; training effect, $F_{2,45} = 3.159$, p = 0.052, training x group interaction, $F_{1,45} = 0.8962$, p = 0.41). Left bottom, average number of errors during reversal training (Mann-Whitney test, p = 0.0301). Middle top, latency to reach the target location (two-way ANOVA: group effect, $F_{1,45} = 5.672$, p = 0.0215; training effect, $F_{2,45} = 3.409$, p = 0.0418, training x group interaction, $F_{1,45} = 0.5787$, p = 0.56). Middle bottom, average latency during reversal training (Mann-Whitney test, p = 0.0208). Right top, path length (two-way ANOVA: group effect, $F_{1,45} = 3.734$, p = 0.0596; training effect, $F_{2,45} = 3.075$, p = 0.056, training x group interaction, $F_{1,45} = 1.03$, p = 0.36). Right bottom, average path length during reversal training (Mann-Whitney test, p = 0.036). * indicates statistically significant.
- (E) Milk reward has no effect on navigation speed (two-way ANOVA: group effect, $F_{1,45} = 0.2218$, p = 0.64; training effect, $F_{2,45} = 1.379$, p = 0.26, training x group interaction, $F_{1,45} = 0.6077$, p = 0.54). Data are presented as mean \pm SEM.
- **Fig. 6.** Appetitive reward occludes ensuing ex vivo DA-LTD within a certain time window.
- (A) Slice recording is made to examine the effect of exogenous DA on synaptic transmission from PP to the DG immediately after the mouse receives a reward of sweetened condensed milk.
- (B) Summary of results obtained from GCs treated with two identical DA perfusions with a 50-min interval (black bars). LTD of PP-driven excitatory postsynaptic currents (EPSCs) induced by the first drug administration is not further increased by the second one. Data represent the EPSC amplitudes

normalized by the mean values before drug perfusion (dotted line) and averaged over 2-min bins for each experiment. Error bars, ±SEM.

- (C) DA fails to induce LTD *in vitro* within a critical time window after milk reward. Summary data of the effects of DA perfusion on GCs in the outer GC layer in slices from control (gray) and milk-treated (black) mice. All recordings were made between 2 and 4 hr after delivery of milk reward. Data are presented in the same manner as in (B).
- (D) Exogenous DA induces LTD again >4 hr after milk reward. Same as in (C) except that all recordings were made more than 4 hr after milk delivery.
- (E) Summary results of the effects of DA perfusion on GFP-labeled adult-generated GCs at 4–6 wpi in slices from control (gray in green) and milk-treated (green) mice. All recordings were made between 2 and 4 hr after delivery of milk reward. Data presented as in (B).
- (F) Same as in (E) except that all recordings were made over 4 hr after milk delivery.
- (G) Comparison of DA actions on PP-elicited responses of mature GCs in brain slices from mice treated with milk (black) and animals intraperitoneally pre-injected with either sulpiride (open box) or SCH 23390 (gray) before milk reward. Data presented as in (B).
- Fig. 7. Region-specific dopaminergic regulation in the hippocampus
- (A) Left, location of stimulating and recording electrodes for extracellular field recordings from SC (red) and TA (blue) pathways in area CA1. A cut was placed between the DG and the CA3 (dotted line) to avoid polysynaptic activation. Right, average traces of 30 consecutive sweeps of fEPSPs in response to SC or TA stimulation recorded before and within 10 min after bath application of DA.
- (B) In comparison to time-matched saline controls (Veh), DA administration (black bar) induces a significant STD in fEPSPs at TA-CA1 synapses but does not affect the strength of SC-CA1 synapses.

Data represent the fEPSP amplitudes normalized against the average of baseline traces (dotted line) and binned over 2-min spans. Error bars, \pm SEM.

- (C) DA attenuates PP- but not A/C-evoked fEPSPs in area CA3. Data presented the same as in (B).
- (D) DA causes an LTD of PP-elicited fEPSPs in the DG.
- (E) Comparison of DA effects on responses to cortical inputs in distinct hippocampal subfields.
- (F) No difference in DA-induced depression of TA-CA1 synaptic responses is observed in slices from control and milk-treated mice.

Figure 1

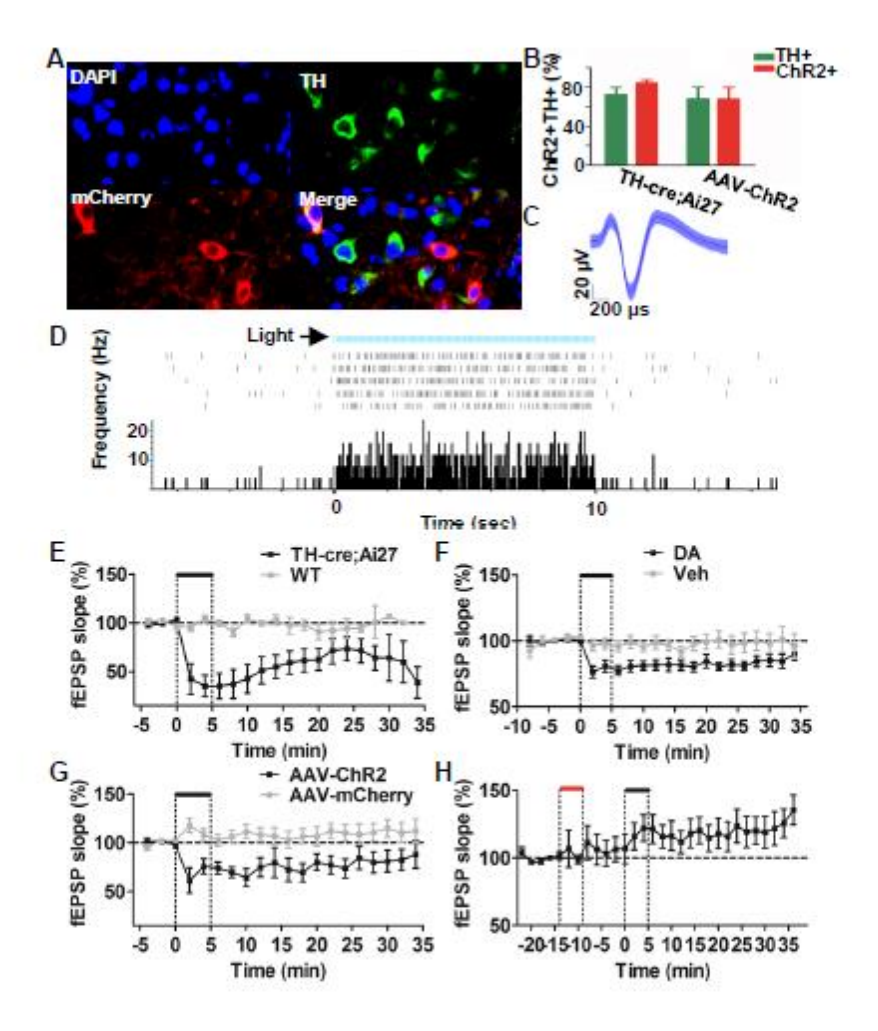


Figure 2

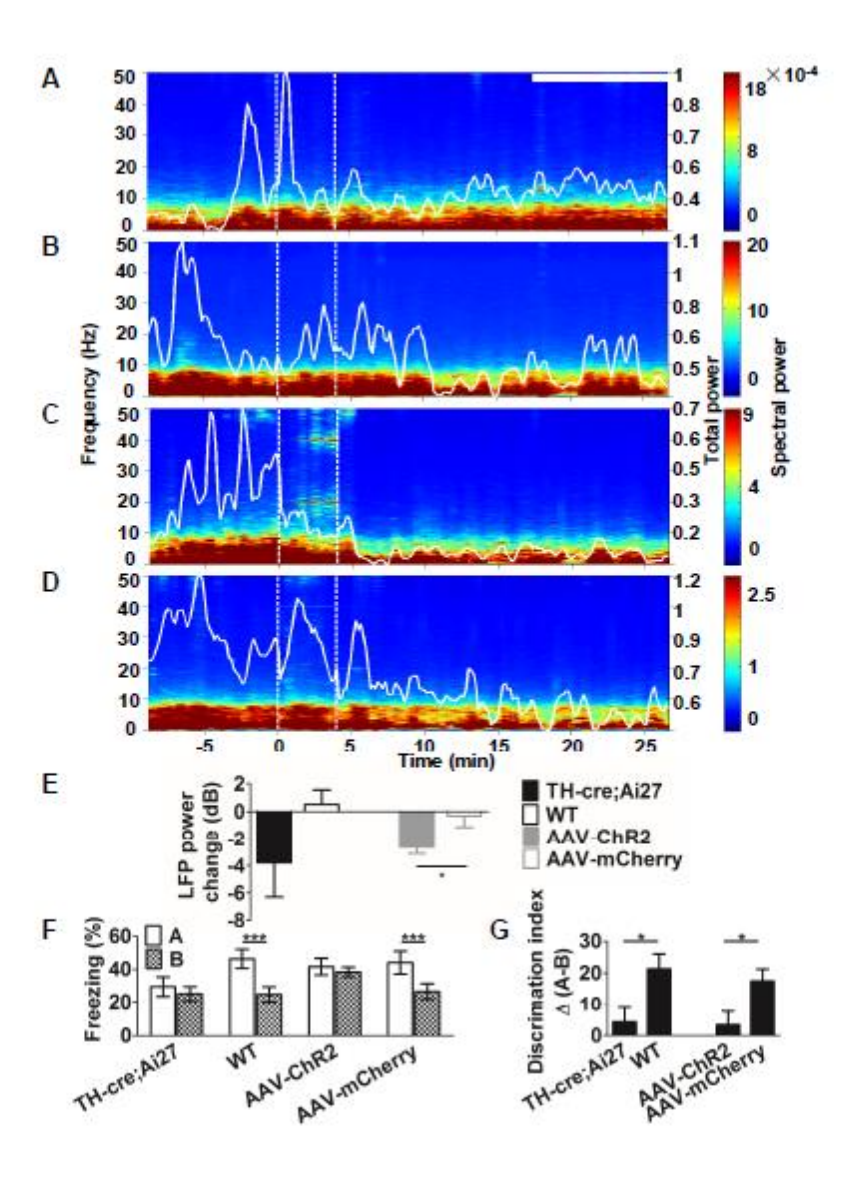


Figure 3

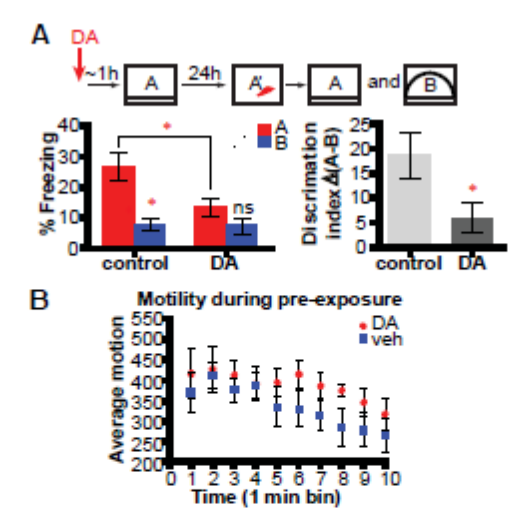


Figure 4

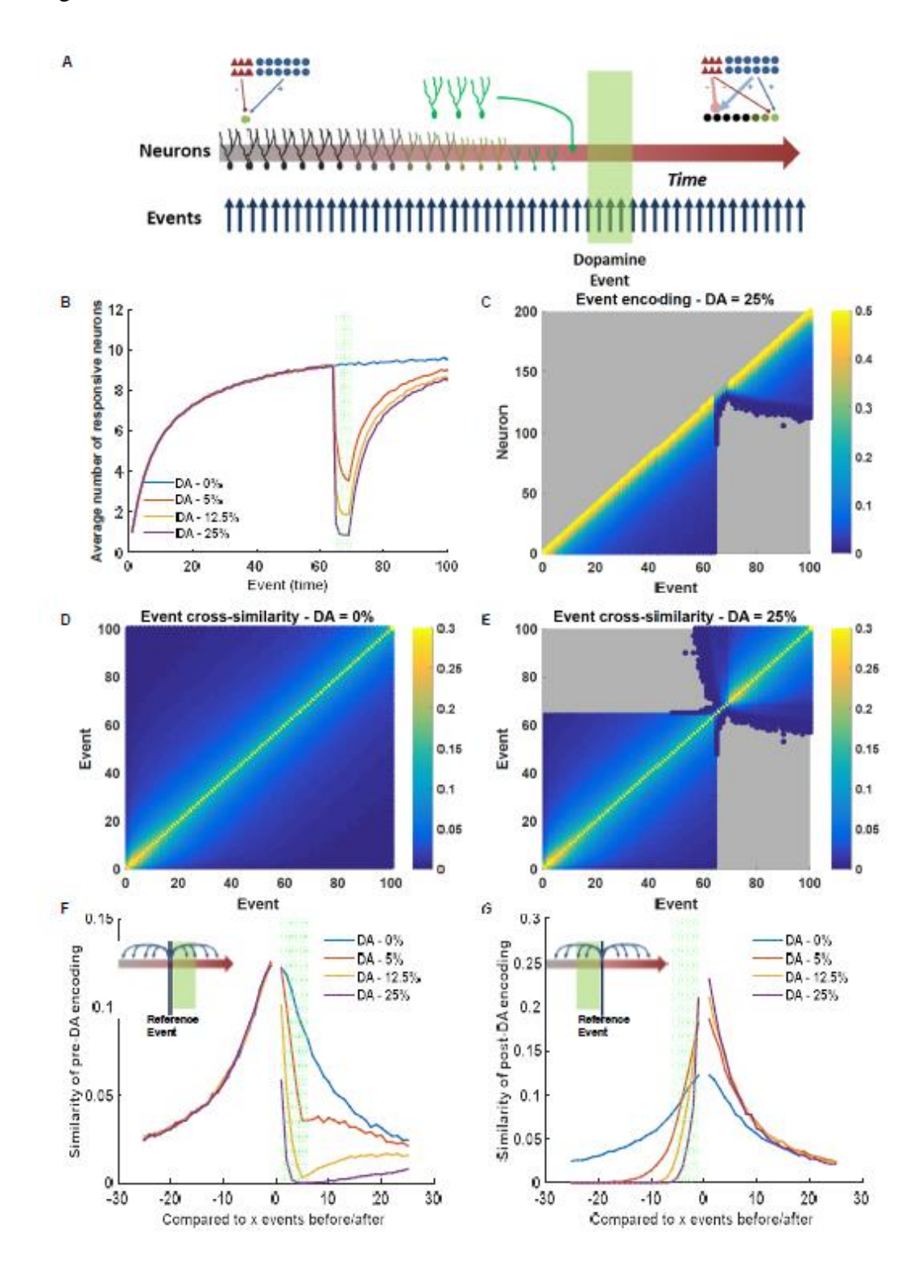


Figure 5

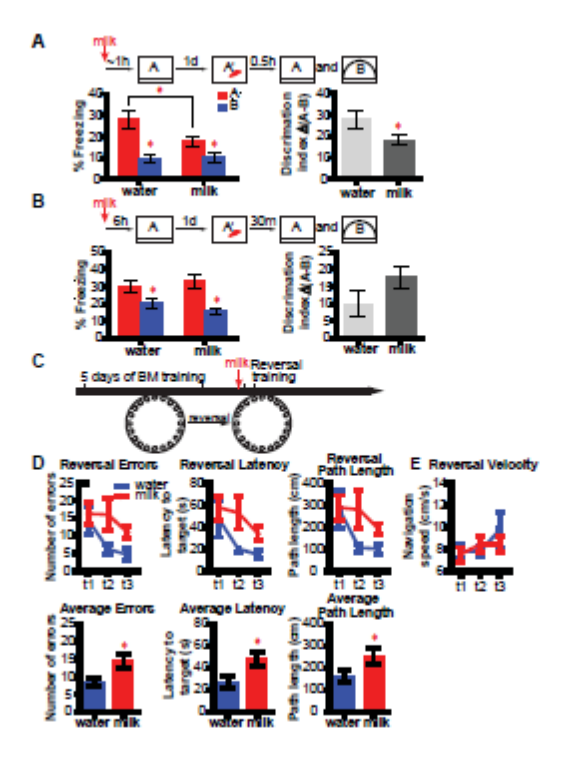


Figure 6

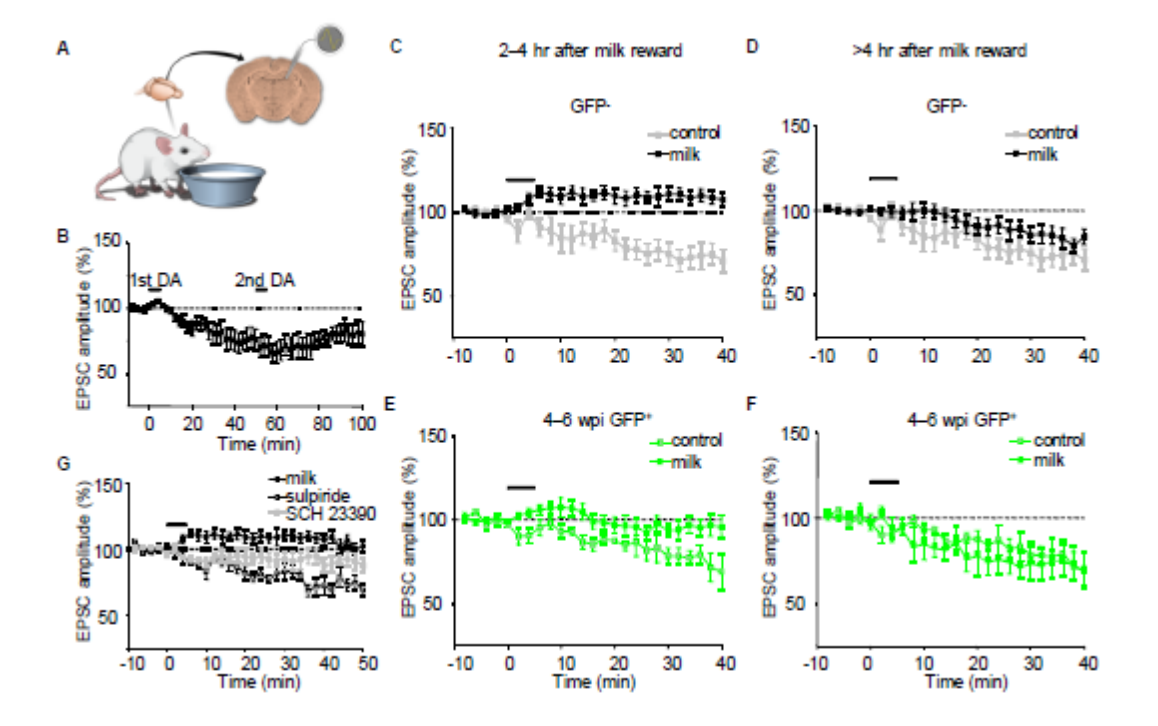
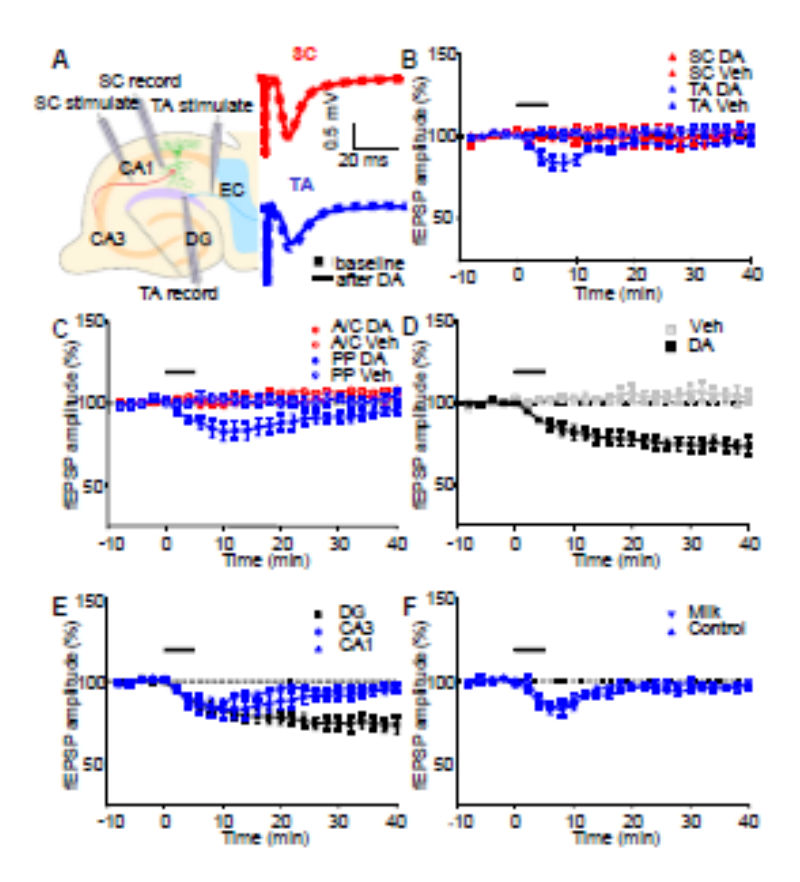


Figure 7



Supporting Information

SI Materials and Methods

Subjects. TH-Cre transgenic mice (45) and Ai27 mice (46) were both maintained as heterozygous in a Specific Pathogen Free (SPF) animal facility and exposed to a 12-h light/dark cycle with food and water provided *ad libitum*. They were crossed to produce a colony of TH-Cre;Ai27 mice in which ChR2 expression was restricted in dopaminergic neurons. WT littermates were used as control. Another cohort of TH-Cre mice was injected with viral vectors encoding Cre-dependent ChR2-mCherry or mCherry only. All the animals (20–35 g, 2–4 months old at the time of surgery) were single housed after surgery and throughout the rest of the experiments. For the milk reward experiments, C57BL/6 female mice were purchased from Harlan and were group housed until one week before the start of the behavioral experiment. After being individually housed for 1–3 days, the animals (3–4 months old) were trained to drink diluted condensed sweetened milk (1:3 milk/water). The sweetened milk was available for 10 min each day for 5 days and the mice were allowed to drink *ad labium* during the training. Typically, the mice drank about 0.7 ml milk in about 5 minutes and spent the rest of the time grooming and resting. All procedures were in strict accordance with institutional guidelines for the care and use of laboratory animals.

Viral labeling. Replication-incompetent retroviruses expressing GFP were used to identify and birthdate adult-generated neurons. The virus was prepared by transfecting plasmids into human embryonic kidney 293T cells. Concentrated virus-containing supernatant $(10^7-10^8 \text{ colony-forming units})$ per ml) was stereotaxically infused into the DG of 6- to 7-week-old female C57BL/6 mice with the following spatial coordinates: anteroposterior = -d/2 mm from bregma (d represents the distance

between bregma and lambda), lateral = -1.6 (if d \leq 1.6 mm) or -1.7 mm, ventral = -1.9 mm from dura. Animals were sacrificed for electrophysiological analysis at the indicated times. For optogenetics experiments, mice were anesthetized with urethane and placed into a stereotaxic frame. A volume of 0.5 μ l AAV-DIO-ChR2-mCherry or control AAV-DIO-mCherry viral vectors (10¹³ colony-forming units per ml, Obio Technology, Shanghai) was bilaterally infused into the VTA (A/P -3.1, M/L 0.5, and D/V - 4.4–4.6) using a 5 μ l Hamilton syringe at the speed of 0.1 μ l/min. At the end of infusion, the syringe needle remained in place for 15 min before retraction.

Histology and imaging. Mice were sacrificed and perfused with 4% paraformaldehyde (PFA) in phosphate buffered saline (PBS). After decapitation, the mouse brains were postfixed overnight and equilibrated in 30% sucrose. Brain tissue was then embedded in O.C.T. and either sectioned into 10-μm slices with an upright Leica cryostat or cut into 40-μm slices with a cooled stage microtome. For immunostaining, slices were incubated with primary antibodies (rabbit anti-TH 1:500, Abcam; mouse anti-DβH 1:300, Millipore) followed by secondary antibodies (Alexa Fluor 488 anti-rabbit IgG 1:1000, Abcam; Alexa Fluor 488 anti-mouse IgG 1:1000, Molecular Probes) and finally DAPI. Immunostained tissue samples were mounted on glass slides and imaged using a Leica TCS SP5-II confocal microscope or Leica SD AF spinning disc confocal system. Image stacks of the DG area were compressed into a single plane using a maximum intensity projection.

Extracellular recording from anesthetic mice. Mice were anesthetized with urethane and mounted on a stereotaxic frame, with body temperature maintained by a 37°C recirculating-water heating pad. For simultaneously recording electrophysiological signals and infusing chemical reagents in close proximity to the electrodes, a cannula (100-μm silica capillary tubing, Polymicro Technologies) and four tetrodes made of four twisted Formvar-coated platinum-iridium wires (17 μm, California Fine Wire) were glued to form a bundle, with the cannula located in the center and connected to a Hamilton syringe that was

filled with drug and mounted in a syringe pump. For optogenetic experiments, an optical fiber (200 µm core diameter, Thorlabs) was affixed to four tetrodes, with the tip of the electrode extending beyond that of the fiber by 500 μ m. The assembly was first targeted at VTA (A/P -3.2 mm, M/L ± 0.3 mm, D/V -4.0 mm) to validate the expression of opsins before being placed in the DG. Light stimulation (5-ms pulses at 20/50 Hz with a power intensity of 13 mW) was applied through the optical fiber connected to a blue laser ($\lambda = 473$ nm, Shanghai Fiblaser Technology Co.) that was controlled by a function generator (AFG3200B, Tektronix). For simultaneous optical stimulation and extracellular recordings in the presence of DA receptor blockers, a cannula and an optic fiber were attached to four tetrodes together. Bipolar tungsten stimulating electrodes (A-M Systems) were placed at the angular bundle of the PP (A/P -3.7-3.8 mm, M/L ± 2.1 mm, D/V -1.8 mm). The cannula and/or optic fiber assembled with multielectrode array was then lowered into the DG (A/P -1.7 mm, M/L ±0.9 mm, D/V -1.8–2.3 mm) to record PP-evoked fEPSPs. All electrode positions were verified histologically following recordings. DA was dissolved in PBS containing 25 μM ascorbic acid to a final concentration of 20 μM. The same volume of vehicle was used as a control in the experiment. The DA antagonist mixture was made in saline containing 10 µM SCH 23390 and 10 µM sulpiride. All drugs were purchased from Sigma.

Extracellular recording from freely moving mice. The mice used for freely moving recordings and subsequent behavior tests were chronically implanted with a custom microdrive that performed simultaneous bilateral light delivery and unilateral electrophysiology measurements. We first made an optetrode by attaching a bundle of eight tetrodes to the optical fiber shaft, with the tetrode tip extending 500 µm beyond the fiber end. The optetrode, together with an additional optic fiber, was then attached to the drive unit with Epoxy (Precision Fiber Products). Surgical procedures were performed under deep anesthesia maintained with 0.5% pentobarbital. The assembled microdrive was secured to the skull using four anchor screws and dental cement, with the optic fiber targeted at the appropriate stereotaxic

coordinates (A/P -1.7 mm, M/L ± 0.9 mm, D/V -1.4–1.6 mm). After the animals recovered from the surgery (~1 week after implantation), the microdrive was advanced gradually to lower the optetrode to desired anatomical locations. Recordings were then performed in the animals' home cage environment. Following in vivo recordings and behavioral experiments, mice were perfused with 4% PFA. Their brains were sectioned to verify the electrode and optic fiber placement, as well as opsin expression within axon terminals in the DG. Mice were excluded if the implantation site was incorrectly positioned. **Data acquisition and analysis.** All electrophysiological recordings in intact *in vivo* preparations were performed using the OmniPlex® D Neural Data Acquisition System (Plexon Inc.). The electrical signal was filtered at 0.05-8,000 Hz, amplified at a gain of 250-5000 and digitized at 40 kHz. Spike sorting was performed with Off-Line Sorter software (Plexon Inc.) utilizing automatic sorting methods and manual checking of single unit isolation. For LFP analysis, signals were down-sampled to a rate of 1000 Hz and low pass filtered at 250 Hz. Time-frequency decomposition of LFP signal was performed using custom code in Matlab and Chronux, an open-source software package for the analysis of neural data. **Contextual fear conditioning.** The fear conditioning paradigm was designed based on immediate shock deficit, a phenomenon referring to the inability of animals to form an association between the conditioning context with an aversive stimulus, such as foot shock, if the stimulus is delivered immediately after the animal is introduced into the context. The immediate shock deficit can be rescued by pre-exposing the animal to the conditioning context (47). Contextual fear conditioning started at least 5 days after optic fiber implantation or milk training and was performed in a conditioning apparatus from Taimeng or Med Associates. The conditioning chambers were located inside sound attenuation boxes. On the first day, mice were allowed to explore the conditioning chamber (context A) with a plastic floor for 10 minutes. The next day, mice received an immediate foot shock (0.72 mA, 2 s) 5 s after being placed into context A', where the plastic floor was removed to expose the wired floor for

shock delivery. Thirty to 60 minutes after shock, the fear behavior of mice was tested by placing them into context A and another context (context B) in a counterbalanced order. Context B was modified from context A by changing the olfactory cues (vanilla extract-scented), the shape of the chamber (an inserted curved plastic board) and distal visual cues (posted on the walls of sound attenuation boxes). Mice were allowed to drink either sweetened milk or water at various points during the behavioral procedure: 40–60 minutes before pre-exposure on the first day, immediately after pre-exposure, 30 minutes before immediate shock, or 30 minutes before testing. All behaviors of the mice were recorded and analyzed by video freeze software (Stoelting ANY-maze or Med Associates).

Barnes maze. The Barnes maze was 91.4 cm (3 feet) in diameter with 20 circular holes around the periphery. The diameter of each hole was 5.1 cm (2 inches). Each hole was connected to a shallow removable plastic box about 2 cm below the maze surface except for one randomly selected hole, which was connected to a hidden escape tunnel. The apparatus was brightly lit. In the initial training phase, mice were trained three trials per day for 5 days. For each trial, an individual mouse was placed into an opaque cylinder in the center of the maze to promote spatial disorientation. Thirty seconds later, the cylinder was removed and the mouse was allowed to explore the maze for three minutes to locate the hidden escape tunnel. The trial ended when the mouse found the escape tunnel or three minutes had elapsed. Once the mouse reached the escape tunnel, it was left there for about 20 seconds. If a mouse failed to locate the escape tunnel, it was gently guided to the escape location and was allowed to stay there for 20 seconds. The position of the escape tunnel remained the same throughout the initial training phase for each individual animal. On the sixth day of training, the escape tunnel was moved to another hole that was 90 degrees from the original position. Two positions were used for the original and the new target locations, which were counterbalanced across mice. Thirty to 60 minutes before training, sweetened milk was provided for one group of mice as a reward. Mice were allowed to drink for 10

minutes. The other group of mice was provided with water as control. Mice were subsequently trained for three trials to locate the new escape position. All trials were recorded with EthoVision software from Noldus. The number of errors made by entering an incorrect hole location was scored by a blinded observer. Errors, the distance traveled before reaching the escape tunnel, and the latency to reach the escape tunnel were used as measurements of spatial learning.

Infusion of DA for behavioral assays. Mice were deeply anesthetized with a mixture of ketamine (100 mg/kg) and xylazine (10 mg/kg), and bilateral 26-gauge cannulas (Plastics One Inc.) were implanted stereotaxically aimed at the DG of the dorsal hippocampus (A/P -1.9, M/L ±1.5, D/V -2.1). A jewelry screw was screwed into the skull next to the cannulas to facilitate the fixation of the cannulas. The cannulas were glued to the skull with a layer of cyanoacrylate gel followed by application of dental cement to secure the implants. Animals were allowed to recover from surgery for at least one week before submitting to any procedures. Infusions were performed using 33-gauge infusion needles that were fitted into the cannulas and were connected to an infusion pump. Infusions (1 μl/side) lasted for 112 seconds and the needles were left in place for an additional 60 seconds to minimize backflow. DA (Sigma) solution (7.5 mg/ml in PBS containing 0.2% ascorbic acid) was made fresh on the day of infusion. PBS containing 0.2% ascorbic acid was used for control infusion.

Computational model. An abstract two-layer neural network model was simulated with individual neurons being represented as binary threshold neurons (i.e., perceptrons or McCullough-Pitts neurons). The input layer had 25,000 excitatory neurons (representing EC) and 6,250 inhibitory neurons (representing local inhibition). The output layer (representing GCs) modeled neurogenesis by gradually adding neurons to the network; initially, the network had zero output neurons with two neurons added per time step up to a total of 200 output neurons. The model did not include feedback or recurrent dynamics, making each output neuron independent of all others. Therefore, it was sufficient to model the

activity and correlations of output neurons without requiring the highly expansive anatomical structure of the biological EC-DG projection. Neurons were initialized with zero synapses and they were gradually matured by adding 100 excitatory and 25 inhibitory synapses per step, up to a total of 5,000 (+) and 1,250 (-) synapses per mature neuron. At each time step, a novel combination of input neurons was activated, driving activity in the output neurons. Neurons fired if excitation surpassed inhibition, and input synapses for active neurons were trained using a simple Hebbian-like learning rule. DA modulation of EC inputs to GCs was simulated by decreasing the activity of EC inputs by a variable fraction (5%, 12.5%, 25%) between time steps 65 and 70. Likewise, NE modulation of EC inputs to GCs was simulated by increasing the activity of EC inputs by a variable fraction (5% or 12.5%) between time steps 65 and 70. Outputs from each time step were compared to outputs of other time steps using normalized dot product (cosyne angle) similarity. A total of 5,000 replicates were performed for each level of DA effect, with averages plotted in Fig. 4.

Retrograde tracing. FG (Fluorochrome Inc.) was dissolved in 0.9% saline to make a 4% (w/v) solution. Seven-week-old female C57BL/6 mice were anesthetized and prepared for surgery in compliance with the Salk Institutional guidelines. The FG solution was then stereotaxically injected into the DG of the animals with the following spatial coordinates: anteroposterior = -d/2 mm from bregma (d represents the distance between bregma and lambda), lateral = -1.6 (if $d \le 1.6$ mm) or -1.7 mm, ventral = -1.9 mm from dura. After a postoperative survival time of two weeks, the animals were perfused transcardially with 0.9% saline followed by 4% paraformaldehyde and then decapitated. The mouse brains were fixed with 4% paraformaldehyde and equilibrated in 30% sucrose. Coronal slices of 40 μ m thickness were cut with a sliding microtome. Polyclonal anti-TH (1:250 dilution; Chemicon) and anti-FG (1:2000, Chemicon) antibodies were used for immunostaining. AF488- and Cy3-conjugated secondary antibodies (1:250 dilution) were used against the primary anti-TH and anti-FG antibodies, respectively. Immunostained

tissue samples were mounted on glass slides, and images were obtained using a Zeiss LSM 710 laser scanning confocal microscope.

Slice electrophysiology. The mice housed in standard cages were anesthetized by isoflurane inhalation. For natural reward experiments, mice were trained to drink sweetened condensed milk in their home cage for 3 or 4 consecutive days and were presented with milk solution immediately before anesthetization. The brains were quickly removed and sliced horizontally using a Leica VT1000S vibratome (200 or 400 μm thickness) in chilled artificial cerebrospinal fluid (ACSF) containing (mM): choline chloride 110, KCl 2.5, NaH₂PO₄ 1.3, NaHCO₃ 25.0, CaCl₂ 0.5, MgCl₂ 7, glucose 20, Naascorbate 1.3, Na-pyruvate 0.6. Slices were recovered at 32°C for >30 min in standard ACSF (NaCl 125, KCl 2.5, NaH₂PO₄ 1.3, NaHCO₃ 25, CaCl₂ 2, MgCl₂ 1.3, Na-ascorbate 1.3, Na-pyruvate 0.6, glucose 10) bubbled with 95% O₂ and 5% CO₂, and subsequently transferred to a recording chamber constantly perfused with ACSF at room temperature. Whole-cell perforated patch recordings were obtained from GCs visually identified by infrared DIC optics and fluorescence, in the presence of 50 µM picrotoxin. The microelectrodes (\sim 3 M Ω) were tip-filled with internal solution composed of K-gluconate 128; KCl 17.5; NaCl 9; MgCl₂ 1; EGTA 0.2; HEPES 10 (pH 7.3) and then back-filled with the same internal solution containing 200 µg/ml amphotericin B. GCs were generally held at a potential of -70 mV in voltage-clamp mode. Input and series resistances were monitored continuously and data were discarded if either of them changed more than 20%. Extracellular field potential recordings were made using microelectrodes (\sim 1 M Ω) filled with external ACSF that did not contain GABA receptor blockers. For both recording configurations, a concentric bipolar tungsten electrode was used for stimulation. All data were obtained using Axopatch 200B patch clamp amplifiers, sampled at 5 kHz and filtered at 2 kHz using a Digidata 1322A analog-digital interface (Molecular Devices).

1. Shohamy D & Adcock RA (2010) Dopamine and adaptive memory. *Trends in cognitive sciences* 14(10):464-472.

- 2. Wise RA (2004) Dopamine, learning and motivation. *Nature reviews. Neuroscience* 5(6):483-494.
- 3. Bao S, Chan VT, & Merzenich MM (2001) Cortical remodelling induced by activity of ventral tegmental dopamine neurons. *Nature* 412(6842):79-83.
- 4. Yagishita S, *et al.* (2014) A critical time window for dopamine actions on the structural plasticity of dendritic spines. *Science* 345(6204):1616-1620.
- 5. Burgess N, Maguire EA, & O'Keefe J (2002) The human hippocampus and spatial and episodic memory. *Neuron* 35(4):625-641.
- 6. Squire LR, Stark CE, & Clark RE (2004) The medial temporal lobe. *Annual review of neuroscience* 27:279-306.
- 7. Frey U, Huang YY, & Kandel ER (1993) Effects of cAMP simulate a late stage of LTP in hippocampal CA1 neurons. *Science* 260(5114):1661-1664.
- 8. Hamilton TJ, et al. (2010) Dopamine modulates synaptic plasticity in dendrites of rat and human dentate granule cells. Proceedings of the National Academy of Sciences of the United States of America 107(42):18185-18190.
- 9. Lemon N & Manahan-Vaughan D (2006) Dopamine D1/D5 receptors gate the acquisition of novel information through hippocampal long-term potentiation and long-term depression. *The Journal of neuroscience : the official journal of the Society for Neuroscience* 26(29):7723-7729.
- 10. Lisman J, Grace AA, & Duzel E (2011) A neoHebbian framework for episodic memory; role of dopamine-dependent late LTP. *Trends in neurosciences* 34(10):536-547.
- 11. McNamara CG, Tejero-Cantero A, Trouche S, Campo-Urriza N, & Dupret D (2014) Dopaminergic neurons promote hippocampal reactivation and spatial memory persistence. *Nature neuroscience*.
- 12. Foerde K & Shohamy D (2011) Feedback timing modulates brain systems for learning in humans. *The Journal of neuroscience : the official journal of the Society for Neuroscience* 31(37):13157-13167.
- 13. Bernabeu R, *et al.* (1997) Involvement of hippocampal cAMP/cAMP-dependent protein kinase signaling pathways in a late memory consolidation phase of aversively motivated learning in rats. *Proceedings of the National Academy of Sciences of the United States of America* 94(13):7041-7046.
- 14. Rossato JI, Bevilaqua LR, Izquierdo I, Medina JH, & Cammarota M (2009) Dopamine controls persistence of long-term memory storage. *Science* 325(5943):1017-1020.
- 15. Kesner RP (2007) A behavioral analysis of dentate gyrus function. *Progress in brain research* 163:567-576.
- 16. Eldridge LL, Engel SA, Zeineh MM, Bookheimer SY, & Knowlton BJ (2005) A dissociation of encoding and retrieval processes in the human hippocampus. *J Neurosci* 25(13):3280-3286.
- 17. Suthana N, Ekstrom A, Moshirvaziri S, Knowlton B, & Bookheimer S (2011) Dissociations within human hippocampal subregions during encoding and retrieval of spatial information. *Hippocampus* 21(7):694-701.
- 18. Zeineh MM, Engel SA, Thompson PM, & Bookheimer SY (2003) Dynamics of the hippocampus during encoding and retrieval of face-name pairs. *Science* 299(5606):577-580.
- 19. Chawla MK, *et al.* (2005) Sparse, environmentally selective expression of Arc RNA in the upper blade of the rodent fascia dentata by brief spatial experience. *Hippocampus* 15(5):579-586.
- 20. Jung MW & McNaughton BL (1993) Spatial selectivity of unit activity in the hippocampal granular layer. *Hippocampus* 3(2):165-182.

- 21. Bakker A, Kirwan CB, Miller M, & Stark CE (2008) Pattern separation in the human hippocampal CA3 and dentate gyrus. *Science* 319(5870):1640-1642.
- 22. Leutgeb JK, Leutgeb S, Moser MB, & Moser EI (2007) Pattern separation in the dentate gyrus and CA3 of the hippocampus. *Science* 315(5814):961-966.
- 23. McHugh TJ, *et al.* (2007) Dentate gyrus NMDA receptors mediate rapid pattern separation in the hippocampal network. *Science* 317(5834):94-99.
- 24. Derrick BE (2007) Plastic processes in the dentate gyrus: a computational perspective. *Prog Brain Res* 163:417-451.
- 25. Lledo PM, Alonso M, & Grubb MS (2006) Adult neurogenesis and functional plasticity in neuronal circuits. *Nat Rev Neurosci* 7(3):179-193.
- 26. Mu Y, Zhao C, & Gage FH (2011) Dopaminergic modulation of cortical inputs during maturation of adult-born dentate granule cells. *The Journal of neuroscience : the official journal of the Society for Neuroscience* 31(11):4113-4123.
- 27. Lammel S, *et al.* (2015) Diversity of transgenic mouse models for selective targeting of midbrain dopamine neurons. *Neuron* 85(2):429-438.
- 28. Harley CW (2007) Norepinephrine and the dentate gyrus. *Progress in brain research* 163:299-318.
- 29. Maher BJ & Westbrook GL (2008) Co-transmission of dopamine and GABA in periglomerular cells. *Journal of neurophysiology* 99(3):1559-1564.
- 30. Tritsch NX, Ding JB, & Sabatini BL (2012) Dopaminergic neurons inhibit striatal output through non-canonical release of GABA. *Nature* 490(7419):262-266.
- 31. Fanselow MS (2000) Contextual fear, gestalt memories, and the hippocampus. *Behavioural brain research* 110(1-2):73-81.
- 32. Deng W, Mayford M, & Gage FH (2013) Selection of distinct populations of dentate granule cells in response to inputs as a mechanism for pattern separation in mice. *eLife* 2:e00312.
- 33. Aimone JB, Deng W, & Gage FH (2011) Resolving new memories: a critical look at the dentate gyrus, adult neurogenesis, and pattern separation. *Neuron* 70(4):589-596.
- 34. Aimone JB, Wiles J, & Gage FH (2009) Computational influence of adult neurogenesis on memory encoding. *Neuron* 61(2):187-202.
- 35. Kesner RP, *et al.* (2014) The role of postnatal neurogenesis in supporting remote memory and spatial metric processing. *Hippocampus* 24(12):1663-1671.
- 36. Rangel LM, *et al.* (2014) Temporally selective contextual encoding in the dentate gyrus of the hippocampus. *Nature communications* 5:3181.
- 37. Ito HT & Schuman EM (2007) Frequency-dependent gating of synaptic transmission and plasticity by dopamine. *Frontiers in neural circuits* 1:1.
- 38. Otmakhova NA & Lisman JE (1999) Dopamine selectively inhibits the direct cortical pathway to the CA1 hippocampal region. *The Journal of neuroscience : the official journal of the Society for Neuroscience* 19(4):1437-1445.
- 39. Buzsaki G (2002) Theta oscillations in the hippocampus. *Neuron* 33(3):325-340.
- 40. Berry SD & Thompson RF (1978) Prediction of learning rate from the hippocampal electroencephalogram. *Science* 200(4347):1298-1300.
- 41. Guderian S, Schott BH, Richardson-Klavehn A, & Duzel E (2009) Medial temporal theta state before an event predicts episodic encoding success in humans. *Proceedings of the National Academy of Sciences of the United States of America* 106(13):5365-5370.
- 42. Arruda-Carvalho M, Sakaguchi M, Akers KG, Josselyn SA, & Frankland PW (2011) Posttraining ablation of adult-generated neurons degrades previously acquired memories. *The*

- *Journal of neuroscience : the official journal of the Society for Neuroscience* 31(42):15113-15127.
- 43. Deng W, Saxe MD, Gallina IS, & Gage FH (2009) Adult-born hippocampal dentate granule cells undergoing maturation modulate learning and memory in the brain. *The Journal of neuroscience : the official journal of the Society for Neuroscience* 29(43):13532-13542.
- 44. Schultz W, Dayan P, & Montague PR (1997) A neural substrate of prediction and reward. *Science* 275(5306):1593-1599.
- 45. Savitt JM, Jang SS, Mu W, Dawson VL, & Dawson TM (2005) Bcl-x is required for proper development of the mouse substantia nigra. *The Journal of neuroscience : the official journal of the Society for Neuroscience* 25(29):6721-6728.
- 46. Madisen L, *et al.* (2012) A toolbox of Cre-dependent optogenetic transgenic mice for light-induced activation and silencing. *Nature neuroscience* 15(5):793-802.
- 47. Landeira-Fernandez J, DeCola JP, Kim JJ, & Fanselow MS (2006) Immediate shock deficit in fear conditioning: effects of shock manipulations. *Behavioral neuroscience* 120(4):873-879.

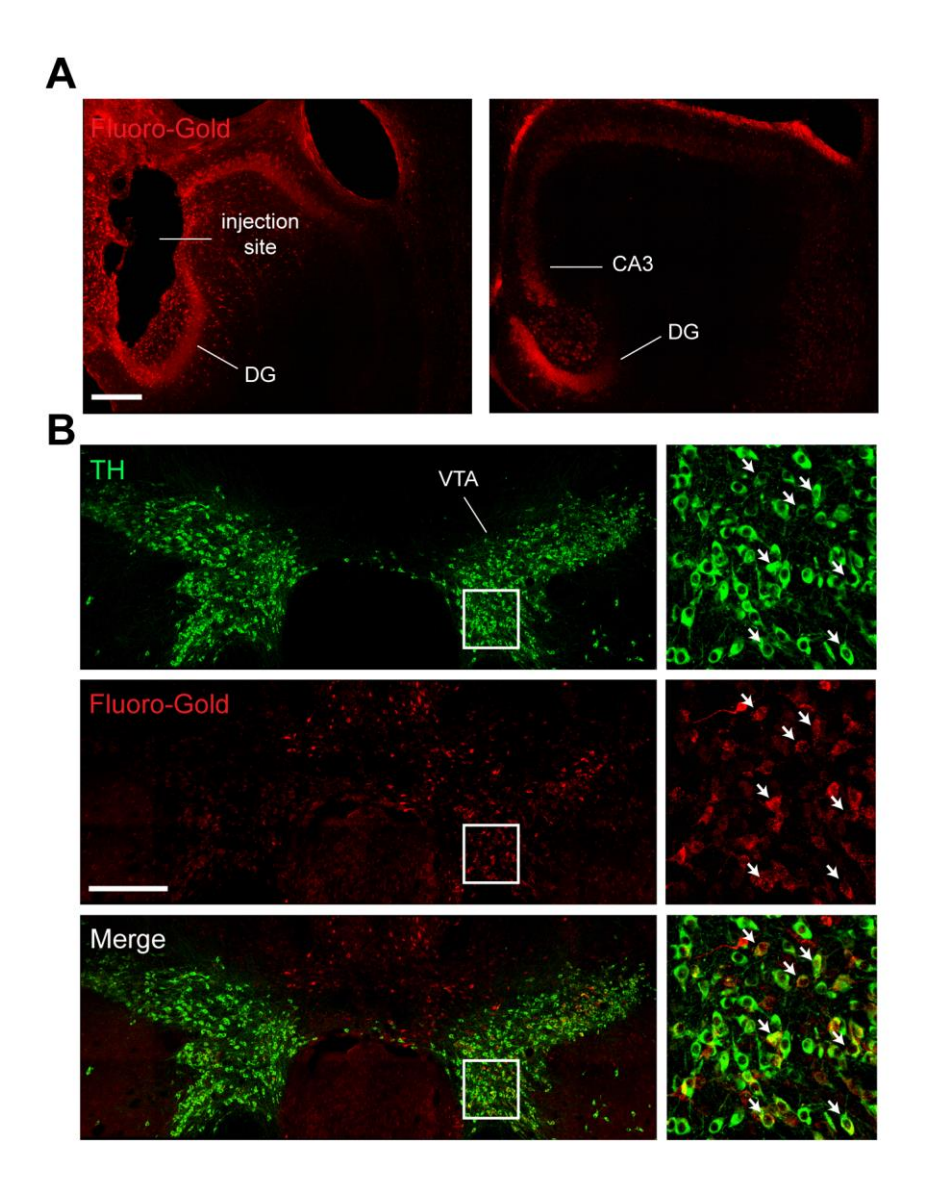


Fig. S1. Photomicrographs of Fluoro-Gold (FG) retrogradely traced neurons double labeled by TH immunohistochemistry

- (A) The left panel depicts FG signals at the injection site in the hippocampus and the right image was taken from a section slightly ventral to the injection site. Scale bar: $200 \ \mu m$.
- (B) Left panels (from top to bottom): sample image of FG-traced neurons, same horizontal section of TH-positive neurons in the midbrain, merged image showing colocalization of FG label with TH staining. Right panels: higher magnification of the boxed region in each left panel. Arrows show double-labeled cells. Scale bar: $500 \, \mu m$.

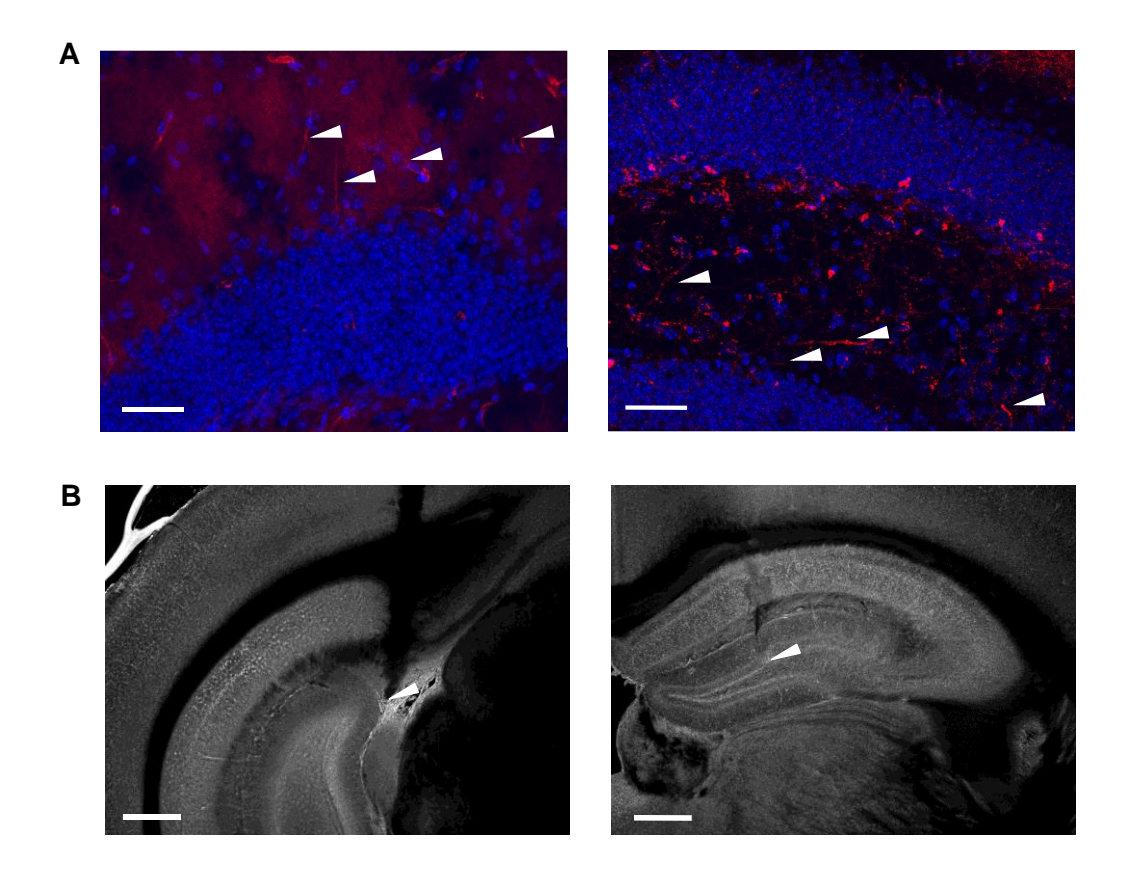


Fig. S2. Stimulation and recording positions in the DG of anesthetized mice (A) Confocal images showing the presence of ChR2-tdTomato-expressing terminals (arrowheads) in the DG. Scale bar: $40 \ \mu m$.

(B) Sample images showing the tracks of stimulating electrode (left panel) and tetrode-optic fiber assembly in the DG (right panel). Arrowheads indicate the electrode tips. Scale bar: $400 \, \mu m$.

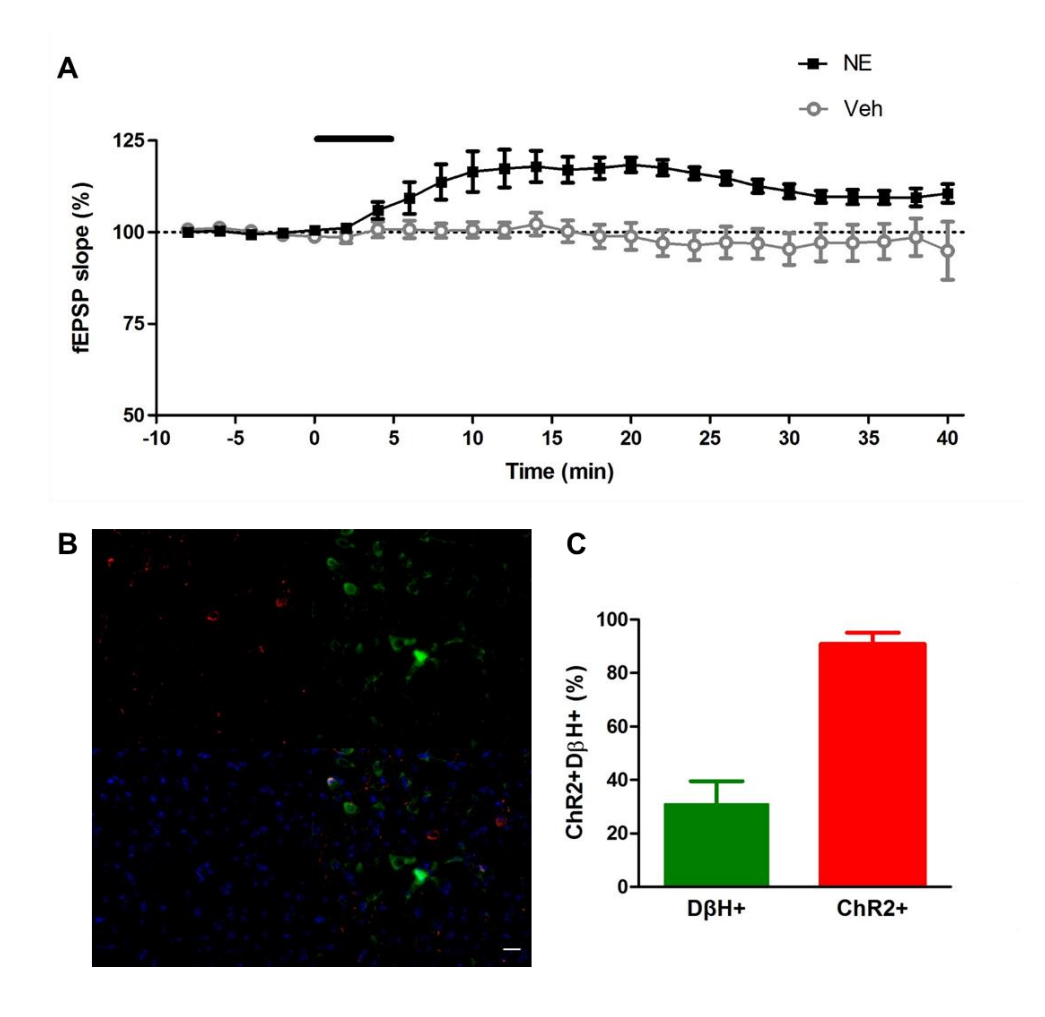


Fig. S3. NE effect and ChR2 expression in noradrenergic neurons

- (A) In comparison to time-matched saline controls, bath application of NE (black bar) induces a small potentiation of PP-evoked fEPSPs in the DG (ANOVA: p < 0.0001; NE group, n = 5; Veh group, n = 4). Data represent the fEPSP slopes normalized against the average of baseline traces (dotted line) and binned over 2-min spans. Error bars, \pm SEM.
- (B) Representative images showing co-expression of ChR2-tdTomato and D β H in the LC of TH-cre;Ai27 mice. Scale bar: 20 μ m.
- (C) Quantification showing the overlap of ChR2+D β H+ cells with D β H+ or ChR2+ cells in the LC. Error bars, SEM.

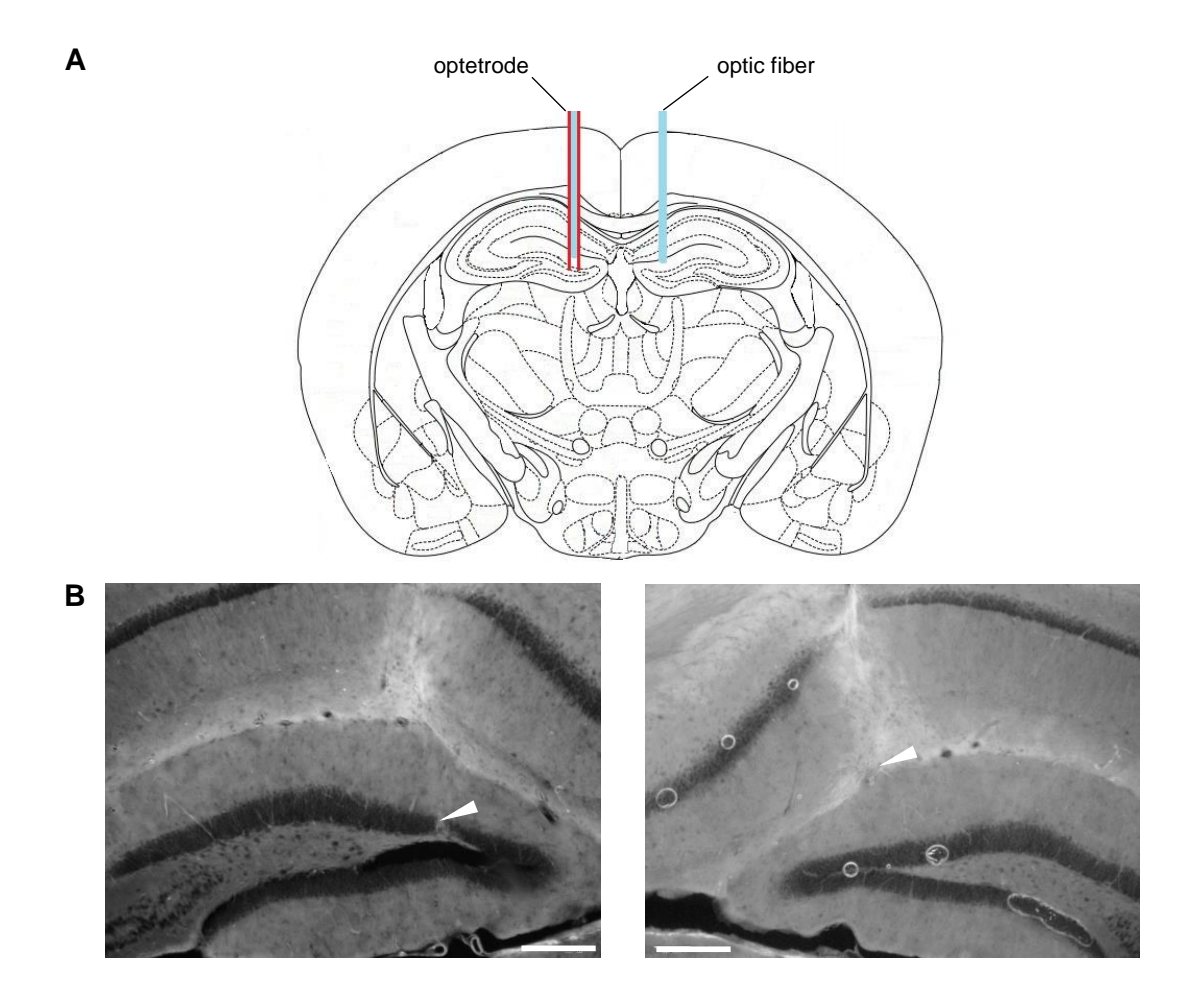


Fig. S4. Sites for optical stimulation and recording in freely moving mice

- (A) Schematic drawing of electrode and optic fiber placement in the DG.
- (B) Sample images showing the tracks of an implanted microdrive consisting of an optetrode (left panel) and an optic fiber (right panel) in the DG. Arrowheads indicate the tips of optetrode and optic fiber. Scale bar: $200 \ \mu m$.

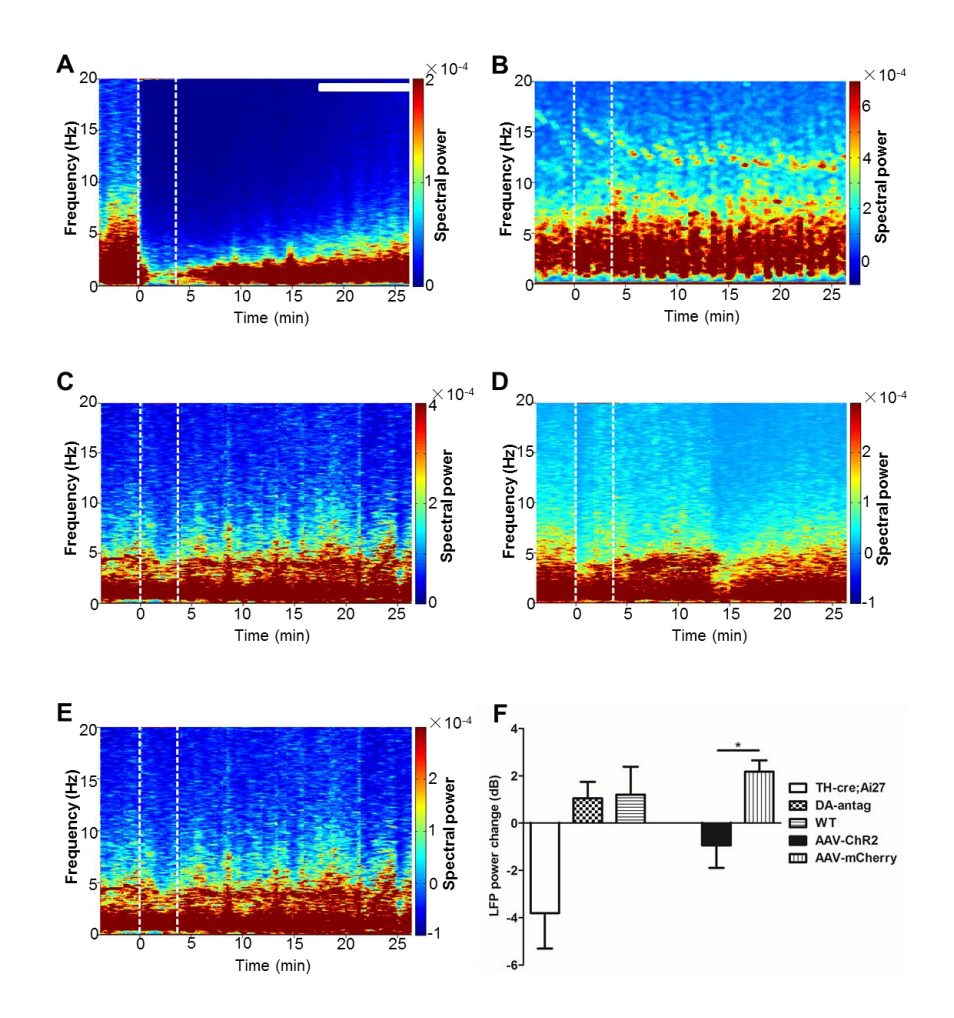


Fig. S5. Optical stimulation induces reduction of theta power in anesthetized animals

- (A) Averaged power spectrogram of LFPs in TH-cre; Ai27 mice exposed to light stimulation. Data are presented in the same manner as in Figure 2A. Horizontal white bar marks the time period used for quantitative comparison of LFP powers between 4 and 12 Hz.
- (B) Pre-treatment with DA antagonists prevents light-induced changes in total power of LFPs in TH-cre; Ai27 mice.
- (C) Averaged power spectrogram of LFPs in WT littermates exposed to light stimulation.
- (D) Averaged power spectrogram of LFPs in TH-Cre mice transduced with AAV-DIO-ChR2-mCherry exposed to light stimulation.
- (E) Averaged power spectrogram of LFPs in TH-Cre mice transduced with AAV-DIO-mCherry exposed to light stimulation.

(F) Histogram showing LFP power (4–12 Hz) change measured during interval indicated in (A) relative to 10-min baseline segment before stimulation (t-test: TH-cre;Ai27 vs. WT, p = 0.077; DA antag vs. WT, p = 0.908; AAV-ChR2 vs. AAV-mCherry, p = 0.016). *p < 0.05.

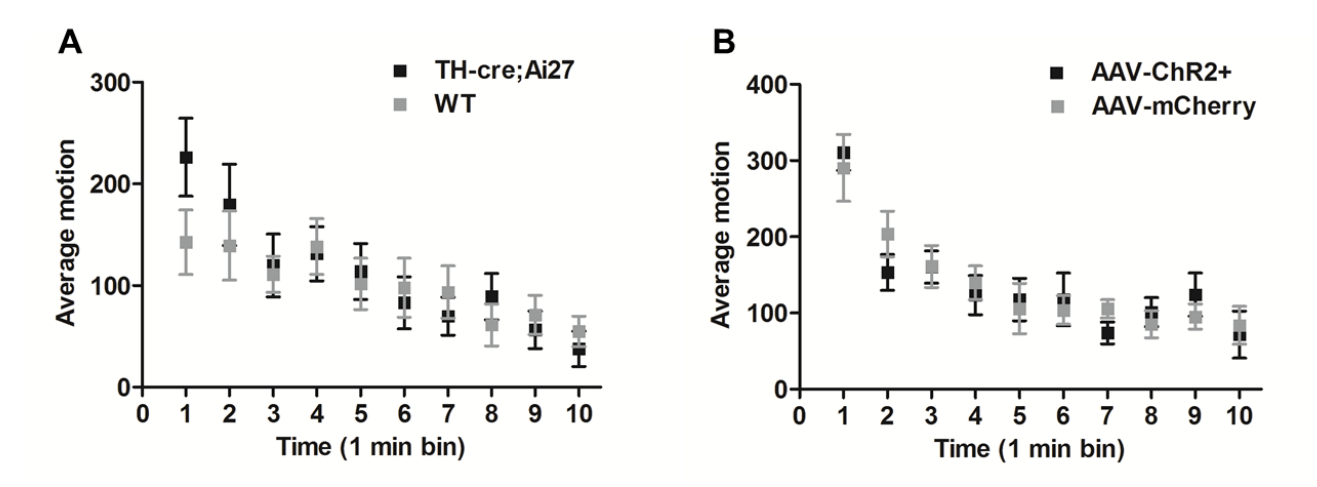


Fig. S6. Photostimulation before the context pre-exposure does not change the exploratory behavior (A) The average motion of TH-cre; Ai27 mice is not significantly different from that of their WT littermates (ANOVA: no significant light x time interaction, $F_{1,9} = 0.7993$, p = 0.6174; no significant light effect, $F_{1,170} = 0.6478$, p = 0.422; main time effect, $F_{9,170} = 5.413$, p < 0.0001; TH-cre; Ai27 group, n = 9; Control group, n = 10).

(B) The average motion of AAV-ChR2 mice is not significantly different from that of AAV-mCherry mice (ANOVA: no significant light x time interaction, $F_{1,9} = 0.4$, p = 0.934; no significant light effect, $F_{1,200} = 0.0032$, p = 0.9552; main time effect, $F_{9,200} = 12.8$, p < 0.0001; AAV-ChR2 group, n = 12; AAV-mCherry group, n = 11).

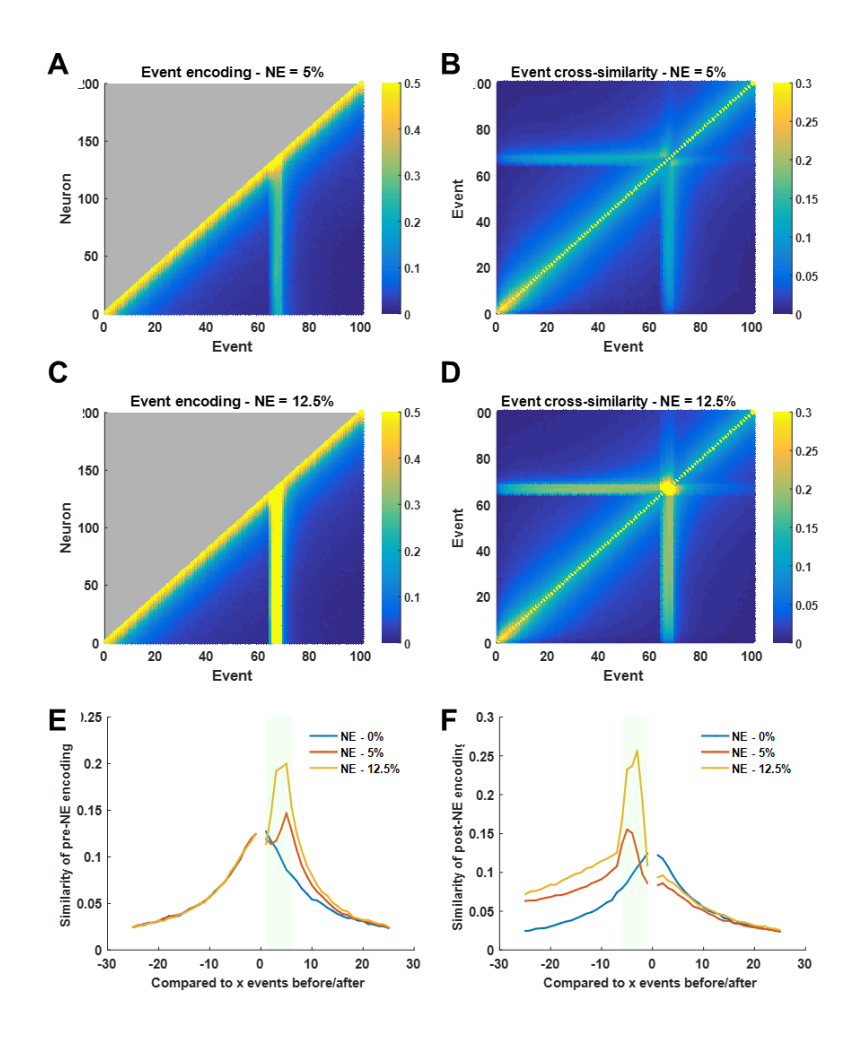


Fig. S7. Implementation of NE in a simple neurogenic two-layer neural network

- (A) Weak NE-induced LTP (+5% strength) broadly activates model DG output.
- (B) Events with 5% NE-induced LTP are weakly correlated with broad range of temporally distant events.
- (C) Moderate NE-induced LTP (+12.5% strength) greatly activates model DG output.
- (D) Events with 12.5% NE-induced LTP are strongly correlated with broad range of temporally distant events. Pre-NE and post-NE events are not differentially encoded using essentially distinct populations of neurons.
- (E) NE-LTP leads to strong correlation of events preceding NE with events during NE.
- (F) Events following NE (shaded area) are more strongly temporally associated with pre-NE events than without NE. In (E) and (F), note the symmetry of associations in the non-NE condition (blue).

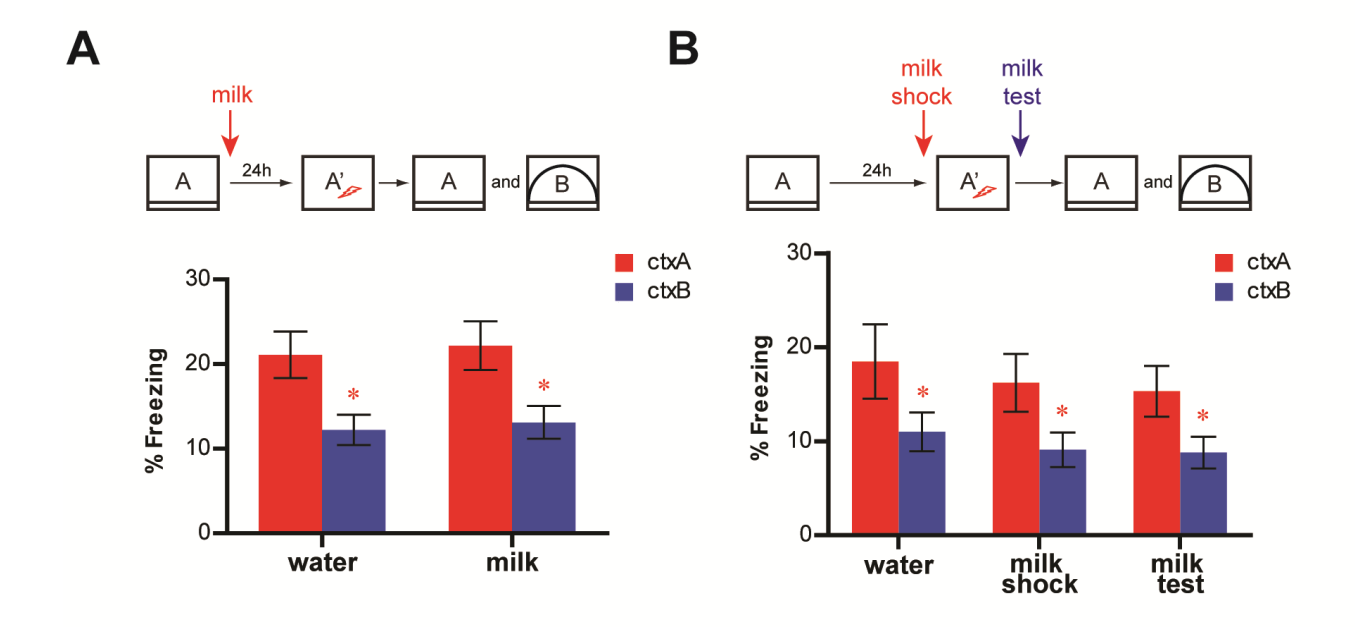


Fig. S8. Reward has no effect on contextual conditioning if reward is received immediately after preexposure, before immediate foot shock or before memory test

- (A) A post-training reward does not affect contextual fear conditioning. Mice treated with sweetened condensed milk perform in the fear test similarly to control mice (ANOVA: no significant treatment x context interaction, $F_{1,1} = 0.002353$, p = 0.96; no significant treatment effect, $F_{1,44} = 0.1221$, p = 0.72; main context effect, $F_{1,44} = 23.85$, p < 0.0001; Bonferroni post hoc test, water group, p < 0.01, n = 24; milk group, p < 0.01, n = 22). * indicates statistical significance.
- (B) Sweetened milk reward received before shock or before testing does not alter fear behavior of mice (ANOVA: no significant treatment x context interaction, $F_{2,1} = 0.03321$, p = 0.96; no significant reward effect, $F_{2,46} = 0.3762$, p = 0.68; main context effect, $F_{1,46} = 21.34$, p < 0.0001; n = 17 for the water group, n = 15 for the milk shock group, n = 17 for the milk test group). * indicates statistical significance.

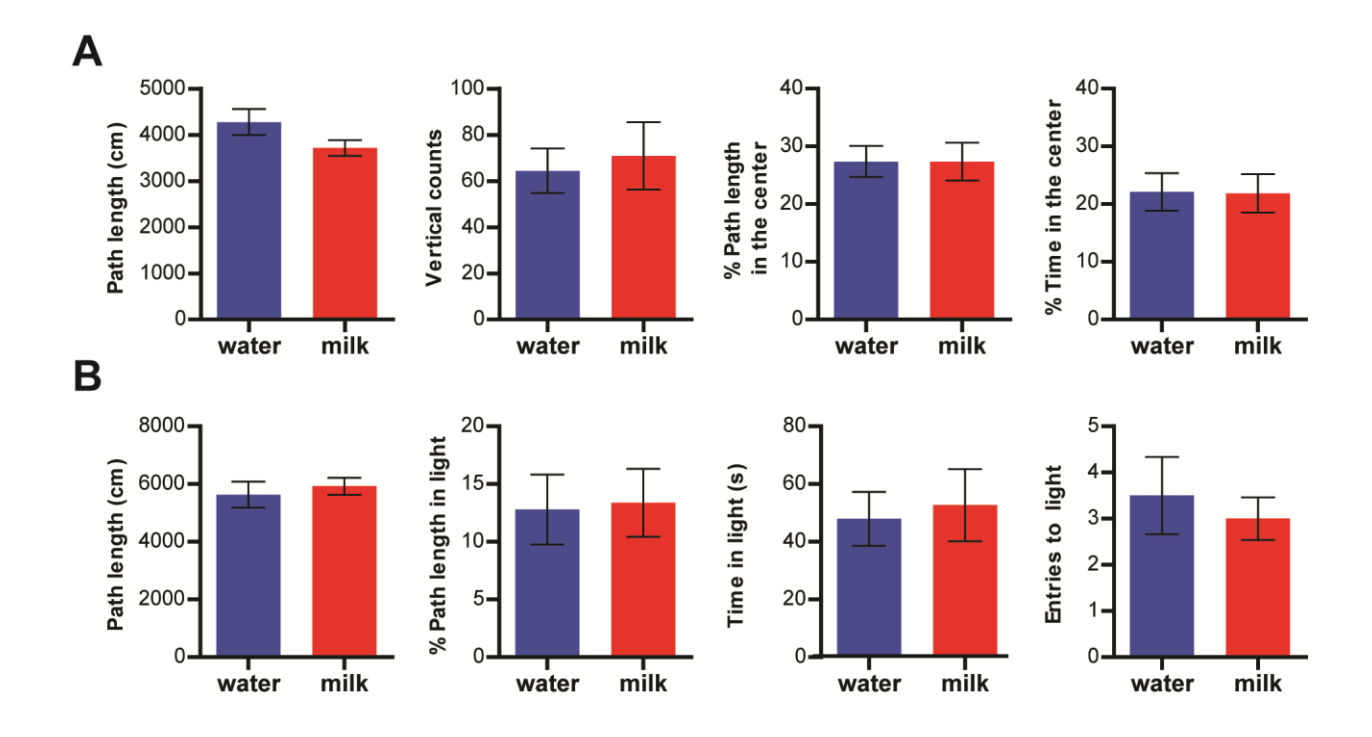


Fig. S9. Pre-test reward does not change the exploratory or anxiety-related behaviors in either the open field test or the light-dark choice test

(A) The open field test. The exploratory behavior, as indicated by ambulatory path length (unpaired t-test, $t_{22} = 1.692$, p = 0.10, n = 12 in each group) and vertical counts (unpaired t-test, $t_{22} = 0.3711$, p = 0.71), is not affected by reward received about one hour before the test. Reward does not affect the anxiety-like behavior, as indicated by the percentage of ambulatory length in the center (unpaired t-test, $t_{22} = 0.0$, p = 1.000) and the percentage of time spent in the center (unpaired t-test, $t_{22} = 0.05182$, p = 0.95).

(B) The light-dark test. The anxiety-like behavior, as indicated by the percentage of ambulatory length in the light compartment (unpaired t-test, $t_{22} = 0.1361$, p = 0.89, n = 12 in each group), the time spent in the light compartment (unpaired t-test, $t_{22} = 0.3029$, p = 0.76), and the number of entries to the light compartment (unpaired t-test, $t_{22} = 0.5222$, p = 0.60), is not affected by reward received about one hour before the test. The exploratory behavior is not affected by reward, as indicated by similar total ambulatory path lengths (unpaired t-test, $t_{22} = 0.5389$, p = 0.59).

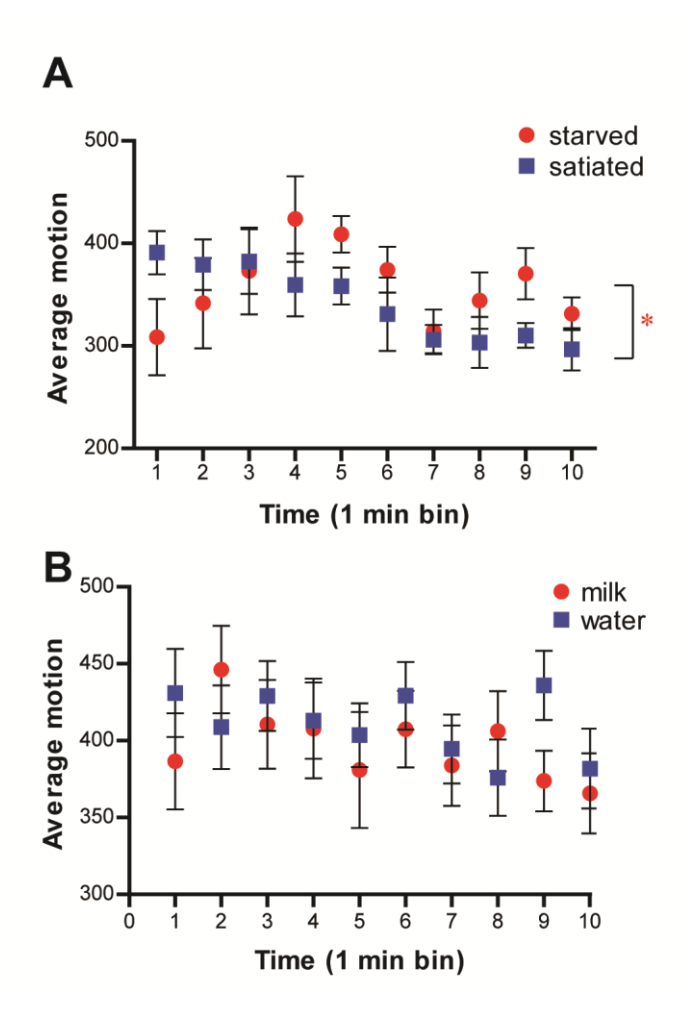


Fig. S10. Pre-learning reward does not change the exploratory behavior of mice during the context pre-exposure

- (A) Changes in satiety affect the exploratory behavior during pre-exposure. The average motion of starved mice is significantly different from that of satiated ones (ANOVA: significant treatment x time interaction, $F_{1,9} = 2.743$, p = 0.0071; no significant treatment effect, $F_{1,90} = 0.3803$, p = 0.55; main time effect, $F_{9,90} = 3.972$, p = 0.0003; starved group, n = 5; satiated group, n = 7). * indicates statistical significance.
- (B) Reward received ~1 hour before learning does not affect exploratory behavior during pre-exposure. Average motion of milk-treated mice is not significantly different from that of water-treated ones (ANOVA: no significant treatment x time interaction, $F_{1,9} = 1.605$, p = 0.11; no significant treatment effect, $F_{1,207} = 0.2018$, p = 0.65; main time effect, $F_{9,207} = 1.993$, p = 0.042; milk group, p = 1.993; water group, p = 1.993.